

Author's Accepted Manuscript

Modelling and investigation of the CD4+ T cells -
macrophages paradox in melanoma
immunotherapies

Raluca Eftimie, Haneen Hamam



www.elsevier.com/locate/jtbi

PII: S0022-5193(17)30077-2
DOI: <http://dx.doi.org/10.1016/j.jtbi.2017.02.022>
Reference: YJTBI8978

To appear in: *Journal of Theoretical Biology*

Received date: 14 February 2016
Revised date: 12 February 2017
Accepted date: 16 February 2017

Cite this article as: Raluca Eftimie and Haneen Hamam, Modelling an investigation of the CD4+ T cells - macrophages paradox in melanoma immunotherapies, *Journal of Theoretical Biology*, <http://dx.doi.org/10.1016/j.jtbi.2017.02.022>

This is a PDF file of an unedited manuscript that has been accepted for publication. As a service to our customers we are providing this early version of the manuscript. The manuscript will undergo copyediting, typesetting, and review of the resulting galley proof before it is published in its final citable form. Please note that during the production process errors may be discovered which could affect the content, and all legal disclaimers that apply to the journal pertain.

Modelling and investigation of the CD4⁺ T cells - macrophages paradox in melanoma immunotherapies

Raluca Eftimie^{1,1}, Haneen Hamam¹

^a*Division of Mathematics, University of Dundee, Dundee DD1 4HN, United Kingdom*

Abstract

It is generally accepted that tumour cells can be eliminated by M1 anti-tumour macrophages and CD8⁺ T cells. However, experimental results over the past 10-15 years have shown that B16 mouse melanoma cells can be eliminated by the CD4⁺ T cells alone (either Th1 or Th2 sub-types), in the absence of CD8⁺ T cells. In some studies, elimination of B16 melanoma was associated with a Th1 immune response (i.e., elimination occurred in the presence of cytokines produced by Th1 cells), while in other studies melanoma elimination was associated with a Th2 immune response (i.e., elimination occurred in the presence of cytokines produced by Th2 cells). Moreover, macrophages have been shown to be present inside the tumours, during both Th1 and Th2 immune responses. To investigate the possible biological mechanisms behind these apparently contradictory results, we develop a class of mathematical models for the dynamics of Th1 and Th2 cells, and M1 and M2 macrophages in the presence/absence of tumour cells. Using this mathematical model, we show that depending on the re-polarisation rates between M1 and M2 macrophages, we obtain tumour elimination in the presence of a type-I immune response (i.e., more Th1 and M1 cells, compared to the Th2 and M2 cells), or in the presence of a type-II immune response (i.e., more Th2 and M2 cells). Moreover, tumour elimination is also possible in the presence of a mixed type-I/type-II immune response. Tumour growth always occurs in the presence of a type-II immune response, as observed experimentally. Finally, tumour dormancy is the result of a delicate balance between the pro-tumour effects of M2 cells and the anti-tumour effects of M1 and Th1 cells.

Keywords: M1 and M2 macrophages, Th1 and Th2 immune cells, B16 melanoma, mathematical approach

2000 MSC: 92C50, 34A34

1. Introduction

2 The anti-tumour role of the immune system has been documented for at least a century,
3 with one of the earliest studies on the role of immune surveillance against transformed cells
4 being published by Ehrlich in 1909 [1]. The last 20-30 years have seen a very rapid increase
5 in the number of experimental studies that investigate the molecular and cellular mechanisms
6 behind the tumour-immune interactions. However, in many cases, the experimental results are
7 contradictory. For example, Mattes et al. [2] investigated the anti-tumour effects of two types of
8 CD4⁺ T cells (Th1 and Th2 cells) on B16 melanoma, and concluded that contrary to the generally
9 accepted idea that the CD4⁺ T cells have only a helper role, they can actually eliminate tumours

10 on their own via the cytokines they produce. Moreover, the authors showed that while the Th1-
 11 tumour interactions led to temporary tumour control followed by tumour escape and growth (see
 12 Figure 1(a)), the Th2-tumour interactions led in the long term to tumour elimination (see Figure
 13 1(a)). In fact, Mattes et al. [2] suggested that tumour elimination in the presence of Th2 cells is
 14 helped by the influx of eosinophils to the tumour site. In addition to eosinophils, the authors also
 15 showed the presence of tumour-infiltrating macrophages (see Figure 1(b)), which seemed to be
 16 associated with tumour growth (but the authors did not investigate the possible anti-tumour/pro-
 17 tumour action of these macrophages). In a later study, Xie et al. [3] showed that the Th1 cells can
 18 actually eliminate B16 melanoma cells (see Figure 2(a)). Kobayashi et al. [4] showed that the
 19 growth of B16F10 cells is associated with a large number of Th2 cells and a high concentration
 20 of IL-4 cytokines (see Figure 2(b)). Moreover, Chen et al. [5] showed that the growth of B16
 21 melanoma cells is associated with a shift from anti-tumour M1 macrophages to pro-tumour M2
 22 macrophages (see Figure 2(c)). (Note that the classification of macrophages into M1 and M2
 23 phenotypes mirrors the Th1 and Th2 nomenclature [6], and despite this strict classification there
 24 is actually a continuum of phenotypes between the M1 and M2 extremes.)

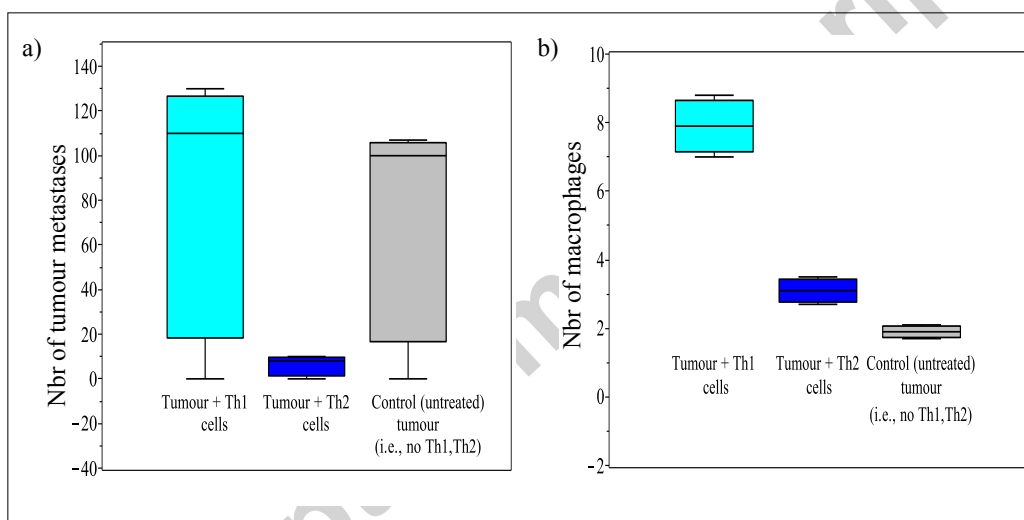


Figure 1: Data approximated and re-drawn from Mattes et al [2], where the authors transfer Th1 cells or Th2 cells into C57BL/6 mice that were previously injected with B16-OVA melanoma cells. a) Number of tumour metastases after the adoptive transfer of Th1 cells, Th2 cells and for the control case (i.e. no treatment with immune cells). b) Number of tumour-infiltrating macrophages following the adoptive transfer of Th1 cells and Th2 cells, and comparison with the number of macrophages in control tumours (with no adoptive transfer of Th1/Th2 cells).

25 The anti-tumour effects of Th1 and Th2 cells are exerted by the cytokines they produce: (i)
 26 the Th1 cells produce type-I cytokines, such as IFN- γ , IL-2, TNF- α and TNF- β [7, 8]; (ii)
 27 the Th2 cells produce type-II cytokines, such as IL-4, IL-5, IL-6, IL-10 and IL-13 [9, 8].
 28 It is usually thought that the type-I cytokines (e.g., IFN- γ , IL-2) have an anti-tumour role [8],
 29 while the type-II cytokines (e.g., IL-10) are generally associated with tumour growth [8]. These
 30 cytokines are not only produced by the Th1/Th2 cells, but also by other cells in the environment:
 31 e.g., macrophages, neutrophils, eosinophils, etc. [8]. In particular, the macrophages can produce,
 32 and respond to, both type-I and type-II cytokines. Classically activated M1 macrophages are

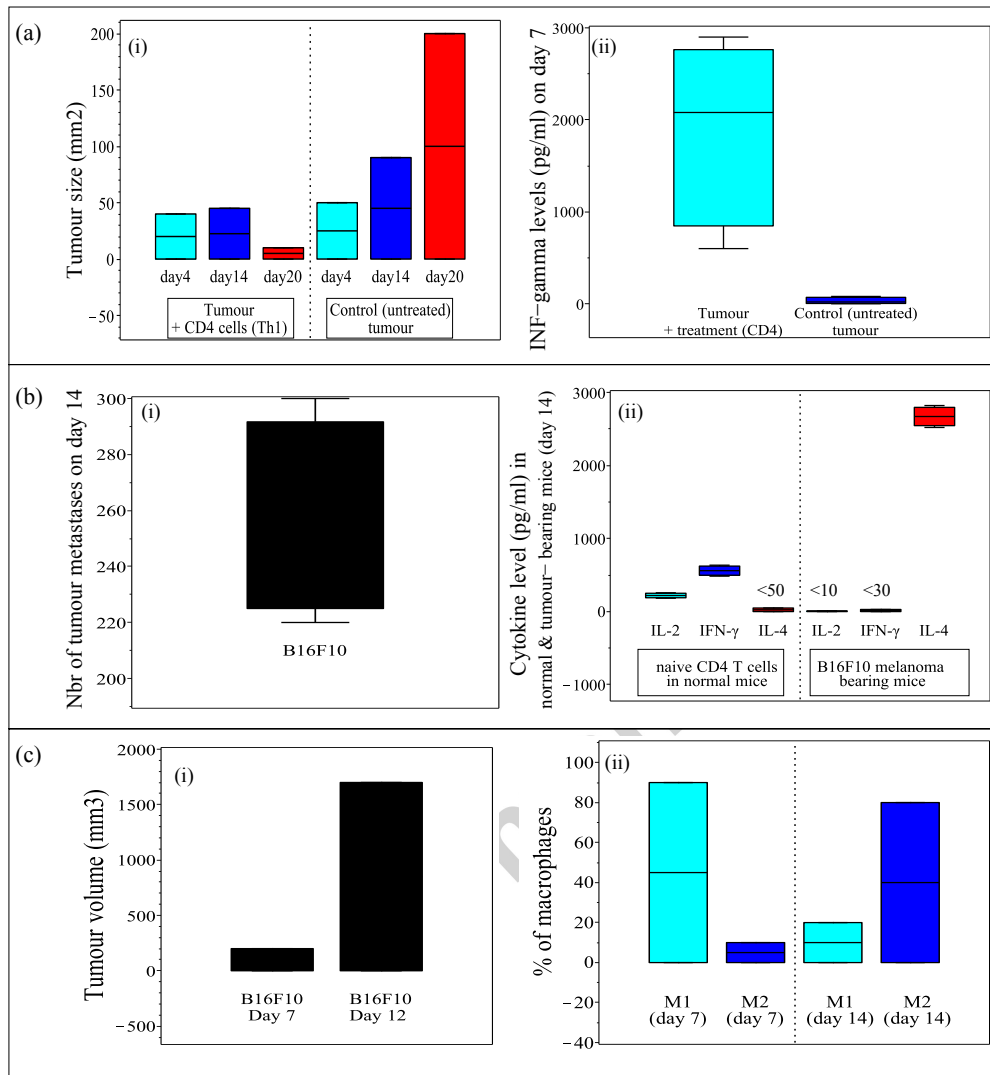


Figure 2: (a) Data approximated and re-drawn from Xie et al [3], where the authors inject $RAG^{-/-}$ mice (which do not have any $CD8^{+}$ T cells, B cells or NKT cells) with B16F10 melanoma cells. Panel (i) shows tumour size on day 20 for mice injected with $CD4^{+}$ T cells and for control mice (with no injection of $CD4^{+}$ T cells); Panel (ii) shows the level of IFN- γ in mice injected with $CD4^{+}$ T cells and in control mice, suggesting that the $CD4^{+}$ T cells that reduce the size of the tumour are actually Th1 cells (which produce high levels of IFN- γ). (b) Data approximated and re-drawn from Kobayashi et al. [4], where the authors inject C57BL/6 mice with B16F10 melanoma cells. Panel (i) shows the number of metastatic colonies on day 14 after injection; Panel (ii) shows the level of IL-2 IFN- γ and IL-4 cytokines produced by naive $CD4^{+}$ T cells in normal mice and in mice injected with B16F10 cells. (c) Data approximated and re-drawn from Chen et al. [5], where the authors inject C57BL/6 mice with B16F10 melanoma cells. Panel (i) shows tumour volume on days 7 and 12 after transfer of tumour cells; Panel (ii) shows the percentage of M1 and M2 macrophages inside the tumour, on days 7 and 14.

33 induced by cytokines such as $\text{IFN-}\gamma$ or $\text{TNF-}\alpha$ [6]. Alternatively activated M2 macrophages
34 are induced by cytokines such as $\text{IL-}4$ and $\text{IL-}13$ [6]. Moreover, the M1 cells are associated
35 with Th1 responses, being involved in resistance against tumours [6]. On the other hand, the
36 M2 cells are associated with Th2 responses, being involved in tumour progression, tissue repair
37 and remodelling [6]. We emphasise here the crosstalk between the Th cells and macrophages via
38 the type-I and type-II cytokines, which might influence the tumour microenvironment (see also
39 Figure 3).

40 The goal of this study is to derive a class of mathematical models that can propose hypothe-
41 ses regarding the apparent paradoxical results in the anti-tumour effects of Th1 and Th2 cells,
42 and M1 and M2 macrophages. We note that in the mathematical literature there are various
43 models investigating different aspects of the interactions between Th1 and Th2 cells, and be-
44 tween M1 and M2 macrophages. For example, the Th1-Th2 dynamics was investigated in the
45 context of cell differentiation and cross-regulation [10, 11, 12], during the immune response to
46 allergens [13] and asthma development [14], during autoimmune diseases [15], following T cell
47 vaccination [16], during bacterial infection in ruminants [7], or in the rejection of cancers such
48 as melanoma [17, 18]. The M1-M2 dynamics was investigated during macrophage activation
49 post-myocardial infarction [19], during wound healing [20], or in the rejection of pancreatic
50 cancer [21]. However, very few mathematical models investigate the interplay between M1/M2
51 macrophages and Th1/Th2 cells during cancer evolution [22]. For example, the study in [22]
52 investigated (numerically and with the help of sensitivity analysis) the influence of the ratio of
53 M1 and M2 macrophages on early and advanced tumour growth, for normal and mutated tu-
54 mour cells. The authors showed that their model can only exhibit tumour growth (i.e., no tumour
55 elimination). Moreover, they showed that while a ratio of $\text{M2:M1} > 1$ can always predict growth
56 towards tumour carrying capacity, a ratio of $\text{M2:M1} < 1$ can lead to either growth towards carrying
57 capacity or growth towards a lower tumour size.

58 In this study, we will investigate the possible mechanisms that could explain the elimination
59 of B16 melanoma by Th2 cells in Mattes et al. [2] and by Th1 cells in Xie et al. [3], and the
60 role played by M1 and M2 macrophages in tumour growth and elimination (given the crosstalk
61 between Th1/Th2 cells and M1/M2 cells via the cytokines they produce; see Figure 3). To this
62 end we develop two mathematical models: (i) a model for the interactions between the Th cells
63 and macrophages alone, which is used to investigate the type-I and type-II immune responses
64 they generate (where we define a *type-I immune response* to be the response dominated by Th1
65 and M1 cells, and a *type-II immune response* to be the response dominated by Th2 and M2 cells);
66 (ii) a model for the interactions between tumour cells, Th cells and macrophages. We show that
67 tumour can be eliminated both in the presence of a type-I immune response and a type-II immune
68 response. Tumour growth is always associated with the presence of a type-II immune response.

69 The structure of this article is as follows. In Section 2 we introduce a mathematical model
70 for the Th cells-macrophages interactions and discuss the long-term behaviour of the model by
71 investigating the number and stability of the steady states. We also investigate numerically the
72 dynamics of this model, and discuss the conditions under which the model displays a type-I
73 or a type-II immune response. In Section 3 we generalise the previous model to incorporate
74 also tumour dynamics. Again, we calculate the steady states and their stability to emphasise
75 the complexity of the new model. We also investigate numerically the short-term and long-term
76 dynamics of the model for tumour-immune interactions, and discuss the parameter values for
77 which we see tumour elimination in the presence of a type-I immune response and in the presence
78 of a type-II immune response. We conclude in Section 3.3 with a summary and discussion of the
79 results.

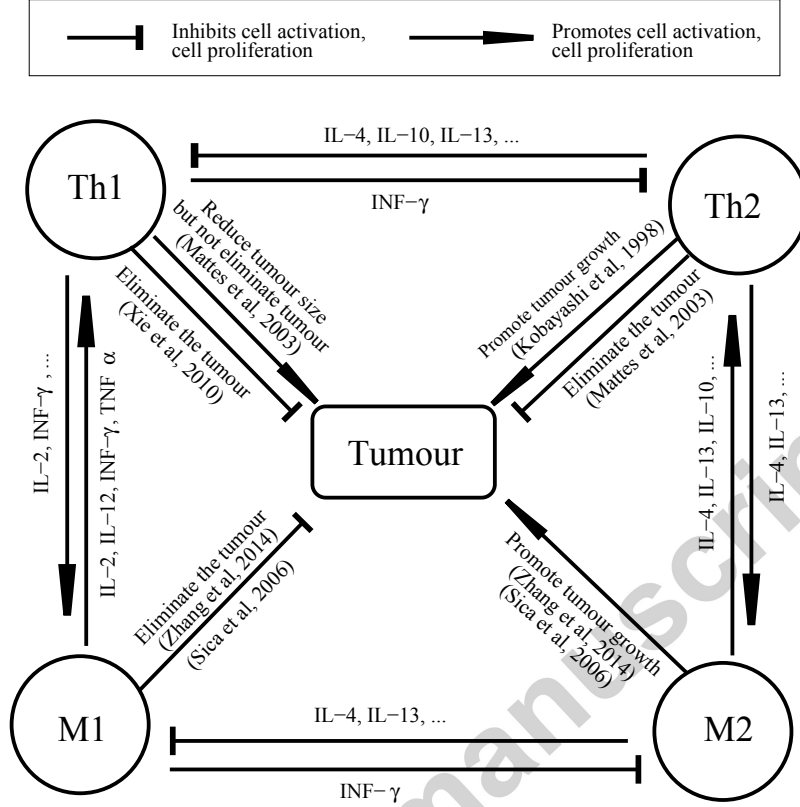


Figure 3: Graphical description of the possible interactions between M1/M2 macrophages, Th1/Th2 cells and tumour cells, via type-I cytokines (e.g. $IFN-\gamma$) and type-II cytokines (e.g. $IL-4$, $IL-13$).

80 2. Modelling the Th1&Th2 and M1&M2 interactions

We first ignore the presence of the tumour, and investigate the dynamics of the interactions between the Th cells and macrophages, following their cross-talk (via cytokines, which we consider implicitly). Thus we define four variables: the density of Th1 cells (H_1), the density of Th2 cells (H_2), the density of M1 macrophages (M_1) and the density of M2 macrophages (M_2). The time-evolution of these variables is given by

$$\frac{dH_1}{dt} = a_{H_1}M_1 + p_{H_1}H_1M_1\left(1 - \frac{H_1 + H_2}{m_1}\right) - e_{H_1}H_1, \quad (1a)$$

$$\frac{dH_2}{dt} = a_{H_2}M_2 + p_{H_2}H_2M_2\left(1 - \frac{H_1 + H_2}{m_1}\right) - e_{H_2}H_2, \quad (1b)$$

$$\frac{dM_1}{dt} = a_{M_1}H_1 + p_{M_1}M_1\left(1 - \frac{M_1 + M_2}{m_2}\right) - e_{M_1}M_1 + r_{M_1}M_2 - r_{M_2}M_1, \quad (1c)$$

$$\frac{dM_2}{dt} = a_{M_2}H_2 + p_{M_2}M_2H_2\left(1 - \frac{M_1 + M_2}{m_2}\right) - e_{M_2}M_2 - r_{M_1}M_2 + r_{M_2}M_1. \quad (1d)$$

81 The following assumptions are incorporated in equations (1):

- 82 • The Th1 cells are activated at a rate a_{H_1} in the presence of IFN- γ cytokines that can be
83 produced by M1 macrophages [23]. These cells grow at a rate p_{H_1} in the presence of
84 type-I cytokines such as IL-2 [24] or IL-12 [25] (which can be also produced by M1
85 macrophages), up to maximum carrying capacity m_1 . The growth term also incorporates
86 the competition between the Th1 and Th2 cells for antigens [7]. Note that high Th2 re-
87 sponses lead to a suppression of Th1 responses and vice-versa, as observed experimentally
88 [7]. The natural death rate of Th1 cells is e_{H_1} [7].
- 89 • The Th2 cells are activated at a rate a_{H_2} in the presence of IL-4 and IL-13 cytokines that
90 can be produced by M2 macrophages [9]. Moreover, the Th2 cells grow at a rate p_{H_2} in
91 the presence of IL-4 [26], up to maximum carrying capacity m_1 . The natural death rate of
92 Th2 cells is e_{H_2} [7].
- 93 • The M1 macrophages are activated at a rate a_{M_1} in the presence of IFN- γ cytokine, pro-
94 duced also by Th1 cells [23, 27]. Also, the M1 cells grow at a rate p_{M_1} via a self renewal
95 process [28], up to a maximum carrying capacity m_2 . The apoptosis rate of M_1 cells is e_{M_1}
96 [29]. Note that M1 macrophages can become M2 macrophages, in the presence of type-II
97 cytokines [30]. We denote by r_{M_1} the re-polarisation rate from M1 to M2 macrophages
98 [19].
- 99 • The M2 macrophages are activated at a rate a_{M_2} in the presence of IL-4, IL-13 (which
100 can be produced by Th2 cells) [27]. Moreover, the M2 cells proliferate in the presence
101 of IL-4 cytokines characteristic to a Th2-environment [31] (hence the proliferation rate
102 $p_{M_2}H_2$), up to a maximum carrying capacity of m_2 cells. (Note that, in contrast to the M2
103 cells, the M1 cells proliferate via self-renewal [28], and thus we do not multiply the p_{M_1}
104 rate with the H_1 variable.) The apoptosis rate of M2 cells is e_{M_2} [29]. Finally, since the M2
105 macrophages can change their phenotype and become M1 macrophages in the presence of
106 type-I cytokines [30], we denote by r_{M_2} the re-polarisation rate from M2 to M1 cells [19].

107 We note here that there are a few studies that suggest the possibility of Th1 \leftrightarrow Th2 re-polarisation
108 based on the environment [32]. However, since this concept of Th re-polarisation is still new, we
109 will not investigate it in this study.

110 A non-dimensionalised version of the model (1) is shown in Appendix C. However, through-
111 out this study we prefer to work with this dimensional model since in the next two sections we
112 will discuss some of the results in the context of dimensional experimental studies. Moreover, the
113 non-dimensionalisation approach does not reduce significantly the number of model parameters.

114 2.1. Steady state and stability

115 Before investigating the long-term behaviour of model (1), we mention that this system has
116 non-negative solutions provided that the initial data are also non-negative (see the discussion in
117 Appendix B). A first step in analysing the long-term dynamics of (1) is to focus on the steady
118 states. The analysis illustrates two types of equilibria:

- 119 1. No immune cells: $(H_1^*, H_2^*, M_1^*, M_2^*) = (0, 0, 0, 0)$. For the parameter values used through-
120 out this study (see Table A.1, and the discussion in Appendix E), the eigenvalues of the
121 Jacobian matrix associated with system (1) are negative at this steady states (see Figure
122 E.16 in Appendix E). Thus, for these parameter values, this immune-free state is stable.
123 A more general discussion about the conditions on the parameter values that allow for
124 stable or unstable zero states can be found in Appendix E.

2. All immune cells present: $(H_1, H_2, M_1, M_2) = (H_1^*, H_2^*, M_1^*, M_2^*)$. There are two such equilibrium points, where the states H_1^* , H_2^* , M_1^* and M_2^* are given implicitly by the following equations:

$$M_1^* = \frac{e_{H_1} H_1^*}{a_{H_1} + p_{H_1} H_1^* \left(1 - \frac{H_1^* + H_2^*}{m_1}\right)}, \quad (2a)$$

$$H_1^* = \frac{e_{M_1} M_1^* + r_{M_2} M_2^* - r_{M_1} M_2^* - p_{M_1} M_1^* \left(1 - \frac{M_2^* + M_1^*}{m_2}\right)}{a_{M_1}}, \quad (2b)$$

$$M_2^* = \frac{e_{H_2} H_2^*}{a_{H_2} + p_{H_2} H_2^* \left(1 - \frac{H_1^* + H_2^*}{m_1}\right)}, \quad (2c)$$

$$H_2^* = \frac{e_{M_2} M_2^* + r_{M_1} M_2^* - r_{M_2} M_1^*}{a_{M_2} + p_{M_2} M_2^* \left(1 - \frac{M_2^* + M_1^*}{m_2}\right)}. \quad (2d)$$

125 For the parameter values chosen in Table A.1, Figure 4 shows that there are two non-zero
 126 steady states (and simple linear stability analysis indicates that one state is stable while
 127 the other state is unstable - see Figure E.16 in Appendix E). Moreover, for the parameter
 128 values used here, we observe that $M_1^* > M_2^*$, and correspondingly $H_1^* > H_2^*$ (see also the
 129 caption of Figure 4 for the exact steady state values). This corresponds to a type-I immune
 130 response that dominates the dynamics of model (1).

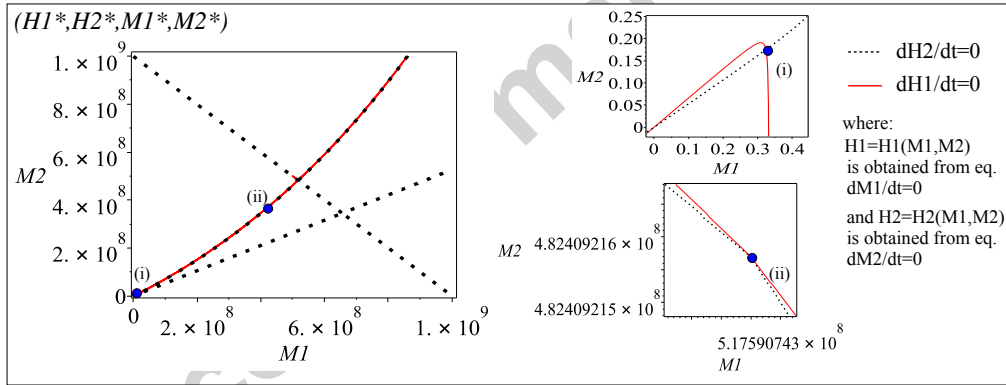


Figure 4: Steady states $(H_1^*, H_2^*, M_1^*, M_2^*)$ for system (1), as shown by the filled circles marking the intersection of nullclines $dH_1/dt = 0$ and $dH_2/dt = 0$. We emphasise that to graph these curves, we first solved $dM_1/dt = dM_2/dt = 0$ for H_1 and H_2 as functions of M_1 and M_2 , and then substituted the expressions for $H_1(M_1, M_2)$ and $H_2(M_1, M_2)$ into the equations for $dH_1/dt = 0$ and $dH_2/dt = 0$. Despite the apparent overlap between the continuous curve for $dH_1/dt = 0$ and the dotted curve for $dH_2/dt = 0$, there are actually only two intersection points (see figures on the right): (i) $M_1^* = 0.324$, $M_2^* \approx 0.175$, $H_1^* = 3.059$, $H_2^* = 0.098$, and (ii) $M_1^* = 5.176 \times 10^8$, $M_2^* \approx 4.824 \times 10^8$, $H_1^* = 5.066 \times 10^7$, $H_2^* = 4.934 \times 10^7$.

131 To investigate the possibility of having also other types of immune responses that dominate the
 132 dynamics (i.e., a type-II response where $M_1^* < M_2^*$ and $H_1^* < H_2^*$; or a mixed type-I/type-II
 133 response where, for example, $M_1^* > M_2^*$ but $H_1^* < H_2^*$) in Figure 5 we present a bifurcation
 7

134 diagram for the ratio of M_1^*/M_2^* and H_1^*/H_2^* steady states (given by equations (2)), as we vary:
 135 (a) the ratio of macrophages re-polarisation rates (r_{M_1}/r_{M_2}) versus the ratio of activation rates for
 136 the Th1 and Th2 cells (a_{H_1}/a_{H_2}), and (b) the ratio of macrophages re-polarisation rates (r_{M_1}/r_{M_2})
 137 versus the ratio of macrophage activation rates (a_{M_1}/a_{M_2}). When we vary a_{H_1}/a_{H_2} in panel (a),
 138 we notice that we can have:

- 139 • a type-I immune response at the overlap between the red (gray on black/white print) sur-
 140 faces, when $r_{M_1}/r_{M_2} \gg 1$ and $a_{H_1}/a_{H_2} \leq 1$;
- 141 • a type-II immune response (at the overlap between the blue surfaces) when $r_{M_1}/r_{M_2} \ll 1$;
- 142 • a mixed type-I/type-II immune response when $r_{M_1}/r_{M_2} \geq 1$ and $a_{H_1}/a_{H_2} \ll 1$.

143 When we vary a_{M_1}/a_{M_2} in panel (b), we notice that we can have either a type-I or a type-II
 144 immune response (since the curves for M_1^*/M_2^* and H_1^*/H_2^* overlap). Details of how we created
 these bifurcation diagrams are presented in Appendix D.

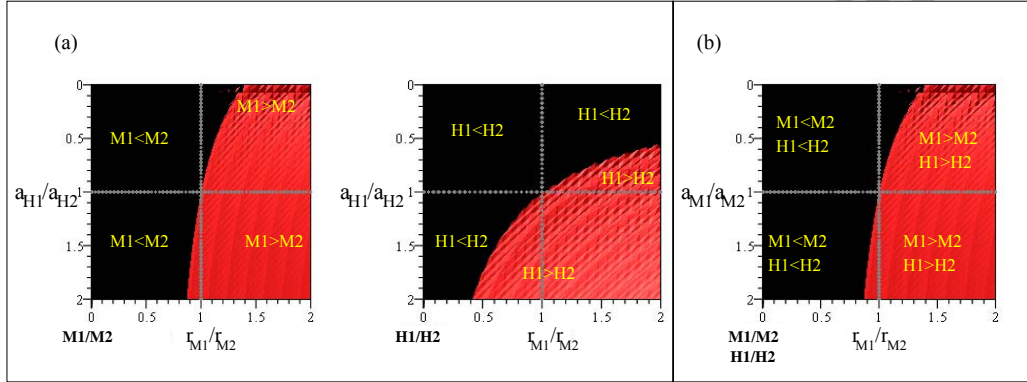


Figure 5: Bifurcation diagram for the ratio of M_1^*/M_2^* and H_1^*/H_2^* steady states (given by equations (2)), as we change the ratio of: (a) r_{M_1}/r_{M_2} versus a_{H_1}/a_{H_2} ; (b) r_{M_1}/r_{M_2} versus a_{M_1}/a_{M_2} . The black surface describes the parameter region where $M_1^*/M_2^* < 1$ or $H_1^*/H_2^* < 1$, while the red surface (gray on black/white print) describes the parameter region where $M_1^*/M_2^* > 1$ or $H_1^*/H_2^* > 1$. Note that for panel (b), the surfaces for H_1^*/H_2^* and M_1^*/M_2^* coincide. A type-I immune response occurs when the red (gray on black/white print) surfaces overlap in each of the panels in (a) and (b). A type-II immune response occurs when the black surfaces overlap in each of the panels (a) and (b).

145

146 2.2. Short- and long-term immune dynamics

147 To investigate numerically the transient and long-term dynamics of macrophages and Th
 148 cells, we use the parameter values described in Table A.1. We assume that antigen is discovered
 149 at time $t = 0$ by the M1 macrophages (which are the primary host defence [33]). So, the initial
 150 values for these simulations are: $M_1(0) = 100$, $M_2(0) = 0$, $H_1(0) = 0$ and $H_2(0) = 0$.

151 In Figure 6 we consider the case $a_{H_1}/a_{H_2} = 0.125 \ll 1$, which leads to an immune response
 152 characterised by $H_1^* < H_2^*$ (since the activation and growth of H_1 and H_2 cells depends on the
 153 magnitudes of a_{H_1} and a_{H_2} ; see also equations (1a)-(1b)). Figure 6(a) illustrates the dynamics
 154 of model (1), when we consider $r_{M_1}/r_{M_2} = 1.8 > 1$ and thus $M_1^* > M_2^*$ (a mixed type-I/type-
 155 II immune response, as predicted by the bifurcation diagram in Figure 5(a)). In regard to the

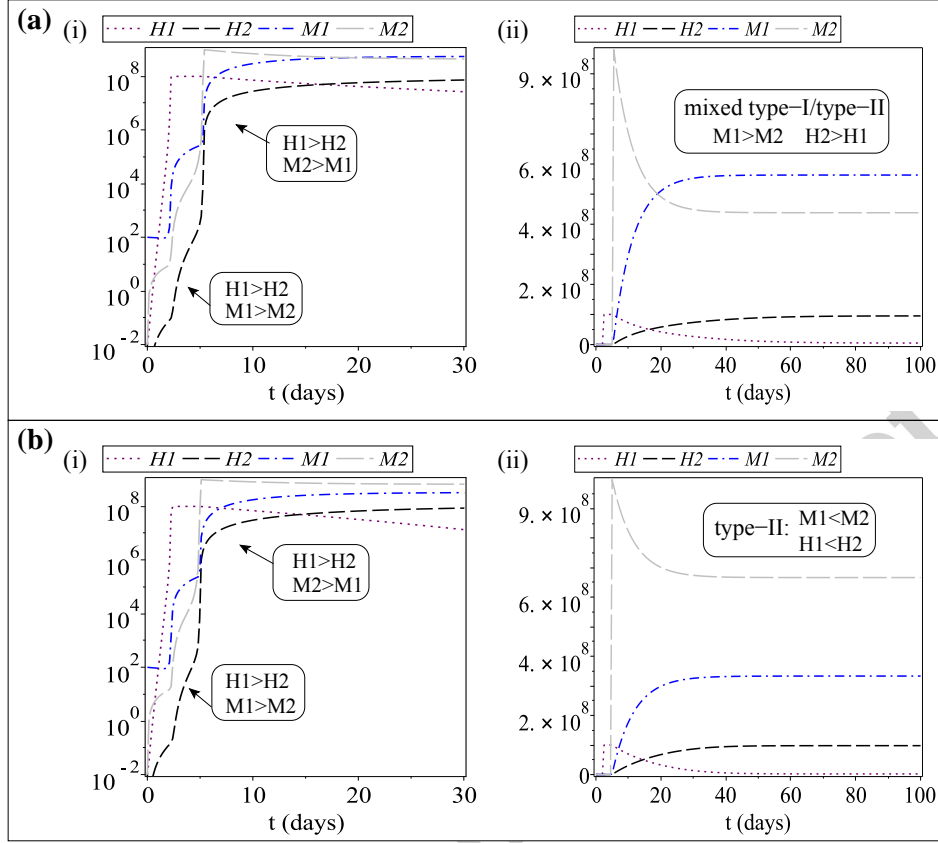


Figure 6: Dynamics of model (1) for $a_{H_1} = 0.001 < a_{H_2} = 0.008$ (which leads to $H_1^* < H_2^*$). (a) Short-term dynamics (panel (i)) and long-term dynamics (panel (ii)) obtained when $r_{M_1} = 0.09, r_{M_2} = 0.05$. (b) Short-term dynamics (panel (i)) and long-term dynamics (panel (ii)) when $r_{M_1} = 0.05, r_{M_2} = 0.08$. For the rest of parameter values see Table A.1.

156 transient immune dynamics: during the first 19 days the Th2 response is lower than the Th1
 157 response, but after day 19 the Th1 response becomes lower than the Th2 response. The large
 158 initial Th1 response leads to a large M1 response. Nevertheless, on day 5, the M2 response
 159 becomes larger than the M1 response. Around day 25, there is a second switch between the
 160 magnitudes of the M1 and M2 responses. Figure 6(b) illustrates the long-term dynamics of
 161 macrophages and Th cells for $r_{M_1}/r_{M_2} = 0.625 < 1$. In this case, the level of M2 macrophages
 162 stays higher than the level of M1 macrophages even during transient times (see panel (b)(i) for
 163 $t \in (5, 30)$; compare this with panel (a)(i) where $M_1 > M_2$ for $t > 25$). Asymptotically, the
 164 solution approaches a steady state with $H_1^* < H_2^*$ and $M_1^* < M_2^*$ (a type-II immune response, as
 165 predicted by the bifurcation diagram in Figure 5(a)).

166 In Figure 7 we consider the case $a_{H_1}/a_{H_2} \gg 1$, which leads to an immune response charac-
 167 terised by $H_1^* > H_2^*$. Figure 7(a) illustrates the dynamics of model (1), when $r_{M_1}/r_{M_2} = 1.8 > 1$
 168 and the long-term dynamics is dominated by a type-I immune response (as predicted by the bi-
 169 furcation diagram in Figure 5(a)). In regard to the transient dynamics, as before we observe a

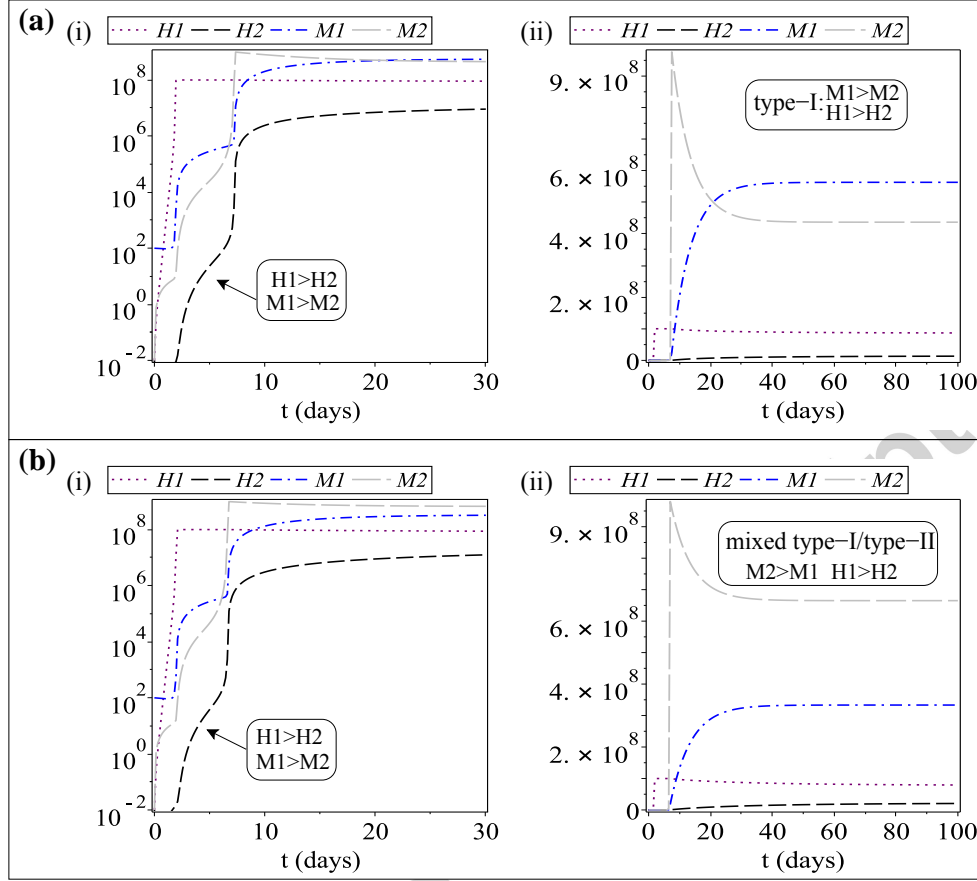


Figure 7: Dynamics of model (1) for $a_{H_1} = 0.008 > a_{H_2} = 0.001$ (which leads to $H_1^* > H_2^*$). (a) Short-term dynamics (panel (i)) and long-term dynamics (panel (ii)) obtained when $r_{M_1} = 0.09, r_{M_2} = 0.05$; b) Short-term dynamics (panel (i)) and long-term dynamics (panel (ii)) obtained when $r_{M_1} = 0.05, r_{M_2} = 0.08$. For the rest of parameter values see Table A.1.

170 double switch in the magnitude of macrophages response. Figure 7(b) illustrates the dynamics
 171 of model (1) for $r_{M_1}/r_{M_2} = 0.625 < 1$. The solution approaches a steady state with $H_1^* > H_2^*$ and
 172 $M_1^* < M_2^*$ (i.e., a mixed type-I/type-II immune response, as predicted by the bifurcation diagram
 173 in Figure 5(a)).

174 Note in Figures 6 and 7 that there are points where the curves have non-continuous deriva-
 175 tives. This is likely a numerical artefact, the result of the number of points used to plot the curves
 176 and the scale of the plot.

177 We conclude that the dynamics of model (1) can be dominated by a type-I, a type-II or a
 178 mixed type-I/type-II immune responses, depending on the ratio r_{M_1}/r_{M_2} and the activation rate
 179 of immune cells. Note that for these simulations, we also varied the macrophages activation
 180 rates (a_{M_1}, a_{M_2}) within the interval $(10^{-4}, 10^{-2})$, but the overall dynamics did not change. We
 181 acknowledge that model dynamics might change if we would vary some of the fixed parameters

182 (i.e., those parameters for which we found values in the literature; see Table A.1).

183 3. Modelling the Th1&Th2 and M1&M2 interactions with tumour cells

Next, we investigate the anti-tumour and pro-tumour effects of M1/M2 macrophages and Th1/Th2 cells. Thus, we consider five variables: the density of tumour cells (T), the density of Th1 cells (H_1), the density of Th2 cells (H_2), the density of M1 macrophages (M_1) and the density of M2 macrophages (M_2). The time-evolution of these variables is given by

$$\frac{dT}{dt} = \alpha T \left(1 - \frac{T}{\beta}\right) - fT - g_{H_1} H_1 T - g_{H_2} H_2 T - g_{M_1} M_1 T + g_{M_2} M_2 T, \quad (3a)$$

$$\frac{dH_1}{dt} = a_{H_1} M_1 + p_{H_1} H_1 M_1 \left(1 - \frac{H_1 + H_2}{m_1}\right) - n_{H_1} H_1 T - e_{H_1} H_1, \quad (3b)$$

$$\frac{dH_2}{dt} = a_{H_2} M_2 + p_{H_2} H_2 M_2 \left(1 - \frac{H_1 + H_2}{m_1}\right) - n_{H_2} H_2 T - e_{H_2} H_2, \quad (3c)$$

$$\frac{dM_1}{dt} = a_{M_1} H_1 + p_{M_1} M_1 \left(1 - \frac{M_1 + M_2}{m_2}\right) - n_{M_1} M_1 T - e_{M_1} M_1 + r_{M_1} M_2 - r_{M_2} M_1, \quad (3d)$$

$$\frac{dM_2}{dt} = a_{M_2} H_2 + p_{M_2} M_2 H_2 \left(1 - \frac{M_1 + M_2}{m_2}\right) + n_{M_2} M_2 T - e_{M_2} M_2 - r_{M_1} M_2 + r_{M_2} M_1. \quad (3e)$$

184 In addition to the assumptions incorporated in model (1), for model (3) we make also the follow-
185 ing assumptions:

- 186 • Tumour cells grow at a rate α , up to a carrying capacity β (which is chosen to correspond to
187 the maximum tumour size allowed for experimental protocols in mice [34]). To model the
188 phenomenological observation that tumour growth slows down as tumour becomes very
189 large and depletes the available nutrients [35], we choose logistic growth. Tumour cells
190 have a very low natural death (i.e., apoptosis) rate f [36]. The Th1 cells kill the cancer
191 cells at a rate g_{H_1} (via IL-2 and IFN- γ); see [37]. Moreover, the tumour cells can be killed
192 by the Th2 cells at a rate g_{H_2} (via IL-4 & IL-13 cytokines that attract eosinophils [2]).
193 Also, M1 macrophages kill tumour cells at a rate g_{M_1} (through the release of tumouricidal
194 products such as NO [38, 39]. Finally, the presence of M2 macrophages increases the
195 proliferation of cancer cells [40]. We denote by g_{M_2} the proliferation rate of cancer cells
196 in the presence of M2 cells. For simplicity, we assumed that all immune cells interact
197 with tumour cells in a linear manner. Under this assumption, the term modelling tumour
198 proliferation can be written as $T(\alpha + g_{M_2} M_2 - \alpha T/\beta)$, suggesting that the presence of M_2
199 cells can increase the maximum tumour size. This seems to be confirmed by experimental
200 studies showing that tumours co-inoculated with M2 macrophages grow much larger than
201 control tumours (see, for example, Fig. 5 in [41]).
- 202 • The Th1 cells can be inactivated by the tumour cells at a rate n_{H_1} [7, 17]. All other rates
203 that control the dynamics of Th1 cells are as described in Section 2.
- 204 • The Th2 cells can be inactivated by the tumour cells at a rate n_{H_2} [7]. All other rates that
205 control the dynamics of Th2 cells are as described in Section 2.
- 206 • The anti-tumour M1 cell population can be reduced, at a rate n_{M_1} , by the tumour cells that
207 secrete pro-tumour cytokines (e.g., IL-10, TGF- β) [6]. All other rates that control the
208 dynamics of M1 macrophages are as described in Section 2.

- 209 • The recruitment of M2 cells at the tumour site is helped by cytokines (e.g., IL-10) and
 210 chemokines (e.g., CCL2) produced by the tumour cells [42]. We denote this recruitment
 211 rate by n_{M_2} . For simplicity, throughout this study we consider $n_{M_2} = n_{M_1}$. All other rates
 212 that control the dynamics of M2 macrophages are as described in Section 2.

213 We emphasise that in model (3), we incorporated only an example of tumour-macrophage-Th
 214 cell interactions. Continuous development of this research area, will likely reveal more types of
 215 interactions among these cells. However, it is not the goal of this article to model detailed dy-
 216 namics of tumour-immune interactions. Rather, we plan to investigate whether the assumptions
 217 incorporated in (3) can explain the paradoxical anti-tumour and pro-tumour immune dynamics
 218 observed experimentally in B16 melanoma cells (as discussed in Section 1).

219 We also note that while there are many other types of tumour growth laws (e.g., exponential,
 220 power, von Bertalanffy, Gompertz or sub-linear) that can fit various experimental data sets, recent
 221 studies suggest that the most appropriate growth laws seem to be dependent on the details of the
 222 experiments and on the particular tumour cell lines [43, 44, 45, 46]. Since the goal of this study
 223 is not to compare in detail our results to various experimental data sets, we decided to focus only
 224 on one law, the logistic growth, and to investigate whether this assumption on tumour growth can
 225 help propose some generic biological mechanisms that can explain the apparent paradox in the
 226 observed anti-tumour immune responses.

227 Before investigating the dynamics of system (3), we note that (3) has non-negative solutions
 228 (see the discussion in Appendix B).

229 3.1. Steady states and stability

230 Next, we study the long-term behaviour of model (3), when the system is at equilibrium. The
 231 existence of four possible equilibrium points (listed below) emphasises the complexity of (3).

- 232 1. No tumour cells and no immune cells: $(T^*, H_1^*, H_2^*, M_1^*, M_2^*) = (0, 0, 0, 0, 0)$.
 233 2. No immune cells, but tumour cells present: $(T^*, H_1^*, H_2^*, M_1^*, M_2^*) = (T^*, 0, 0, 0, 0)$, with $T^* =$
 234 $\beta(1 - f/\alpha)$.
 235 3. No tumour cells and all immune cells present: $(T^*, H_1^*, H_2^*, M_1^*, M_2^*) = (0, H_1^*, H_2^*, M_1^*, M_2^*)$
 236 where H_1^*, H_2^*, M_1^* and M_2^* are described in Section 2.1. As before, there are two such states.
 237 4. Presence of all immune and tumour cells: $(T^*, H_1^*, H_2^*, M_1^*, M_2^*)$, where T^*, H_1^*, H_2^*, M_1^* and
 238 M_2^* are given implicitly by the following equations:

$$T^* = \beta \left(1 - \frac{g_{H_1} H_1^* + g_{H_2} H_2^* + g_{M_1} M_1^* - g_{M_2} M_2^* + f}{\alpha} \right), \quad (4a)$$

$$M_1^* = \frac{n_{H_1} H_1^* T^* + e_{H_1} H_1^*}{a_{H_1} + p_{H_1} H_1^* \left(1 - \frac{H_1^* + H_2^*}{m_1} \right)}, \quad (4b)$$

$$H_1^* = \frac{n_{M_1} M_1^* + e_{M_1} M_1^* + r_{M_2} M_1^* - r_{M_1} M_2^* - p_{M_1} M_1^* \left(1 - \frac{M_2^* + M_1^*}{m_2} \right)}{a_{M_1}}, \quad (4c)$$

$$M_2^* = \frac{n_{H_2} H_2^* T^* + e_{H_2} H_2^*}{a_{H_2} + p_{H_2} H_2^* \left(1 - \frac{H_1^* + H_2^*}{m_1} \right)}, \quad (4d)$$

$$H_2^* = \frac{e_{M_2} M_2^* + r_{M_1} M_2^* - r_{M_2} M_1^* - n_{M_2} M_2^*}{a_{M_2} + p_{M_2} M_2^* \left(1 - \frac{M_2^* + M_1^*}{m_2} \right)}. \quad (4e)$$

239 For the parameter values shown in Table A.1, there are three such steady states that are real
 240 and positive (see Figure E.18 in Appendix E), and their stability is illustrated in Figure
 241 E.19(e)-(g).

242
 243 As in Section 2.1, we are now interested in investigating the parameter space where tumour
 244 growth and elimination occurs in the presence of a type-I immune response, a type-II re-
 245 sponse or a mixed response. Thus, we focus on the two steady states with non-zero immune
 246 responses. Since the steady state $(0, H_1^*, H_2^*, M_1^*, M_2^*)$ is similar to the state investigated in Fig-
 247 ure 5, we can conclude that tumour elimination can occur in the presence of a type-I response,
 248 a type-II response, or a mixed type-I/type-II response. We will return to this aspect in Section
 249 3.2, when we will investigate numerically the long-term dynamics of system (3).

250 For the tumour-immune coexistence state $(T^*, H_1^*, H_2^*, M_1^*, M_2^*)$, let us first investigate the pa-
 251 rameter values for which $T^* > 0$, which is equivalent (from (4a)) with solving the following
 252 equation for $T^* > 0$:

$$\alpha - T^* \frac{\alpha}{\beta} - f - g_{H_1} H_1^* - g_{H_2} H_2^* - g_{M_1} M_1^* + g_{M_2} M_2^* = 0. \quad (5)$$

253 Note in equations (4c)-(4e) that $H_{1,2}^*$ can be expressed in terms of $M_{1,2}^*$. In addition, we can
 254 make the the assumption that $M_1^* + M_2^* \approx m_2$ (assumption supported by the numerical results;
 255 see Figures 10 – 12). This allows us to re-write the condition for the existence of the state
 256 $T^* > 0$ as

$$\frac{\alpha}{\beta} T^* = \alpha - f - \frac{g_{H_1} a_{H_1} m_2 (M)}{(n_{H_1} T + e_{H_1})(1 + M)} - \frac{g_{H_2} a_{H_2} m_2}{(n_{H_2} T^* + e_{H_2})(1 + M)} - g_{M_1} \left(m_2 - \frac{m_2}{1 + M} \right) + \frac{g_{M_2} m_2}{1 + M}, \quad (6)$$

257 where $M = M_1^*/M_2^*$. We graph this equation in Figures 8 (for lower g_{M_1} : $g_{M_1} = 6 \times 10^{-9}$) and
 258 Figure 9 (for higher g_{M_1} : $g_{M_1} = 6 \times 10^{-8}$), to study the changes in the parameter space where
 259 $T^* > 0$, as we vary g_{M_2} , g_{H_1} and g_{H_2} .

260 In Figure 8, we notice that for low g_{M_2} values (see panels (a),(a'); where $g_{M_2} = 2.3 \times 10^{-10}$),
 261 the existence of a tumour-immune coexistence state requires $M = M_1^*/M_2^* \ll 1$ and $H =$
 262 $H_1^*/H_2^* \ll 1$, which is equivalent to a type-II immune response. Increasing g_{M_2} (see panels
 263 (b),(b'); where g_{M_2} is increased 30 times, to $g_{M_2} = 6.9 \times 10^{-9}$) can increase the values of
 264 the ratio M_1^*/M_2^* for which $T^* > 0$ can exist. These results suggest that, for the g_{M_2} values
 265 investigated in this study (panels (a),(a')), whenever tumours grow they are accompanied by
 266 a type-II immune response. However, for very large g_{M_2} values, tumours can exist also for
 267 $M > 1$ and $H > 1$ (see panels (b),(b')). This result suggests that there could be fewer M2
 268 cells compared to M1 cells, but if these cells secrete large amounts of type-II cytokines, they
 269 can skew the tumour microenvironment in favour of tumour sustenance and growth. (We will
 270 return to this hypothesis in the Discussion section.) We also need to emphasise here that an
 271 increase in g_{H_1} (from 4.2×10^{-9} in panels (a),(b), to 1.26×10^{-7} in panels (a'),(b')) reduces
 272 the parameter space over which we can expect tumour-growth in the presence of a type-I
 273 response.

274 In Figure 9 we notice that the 10-fold increase in g_{M_1} (from $g_{M_1} = 6 \times 10^{-9}$ in Figure 8 to
 275 $g_{M_1} = 6 \times 10^{-8}$ here) has two main effects: (i) forces $T^* > 0$ to exist mainly during a type-II
 276 response, and (ii) induces the requirement for much higher g_{M_2} values for tumour persistence
 277 in the presence of a type-I response (i.e., at least a 150-fold increase in g_{M_2} ; see panels (b),(b'),
 278 where only a mixed type-I/type-II response was obtained after a 126-fold increase in g_{M_2}). We

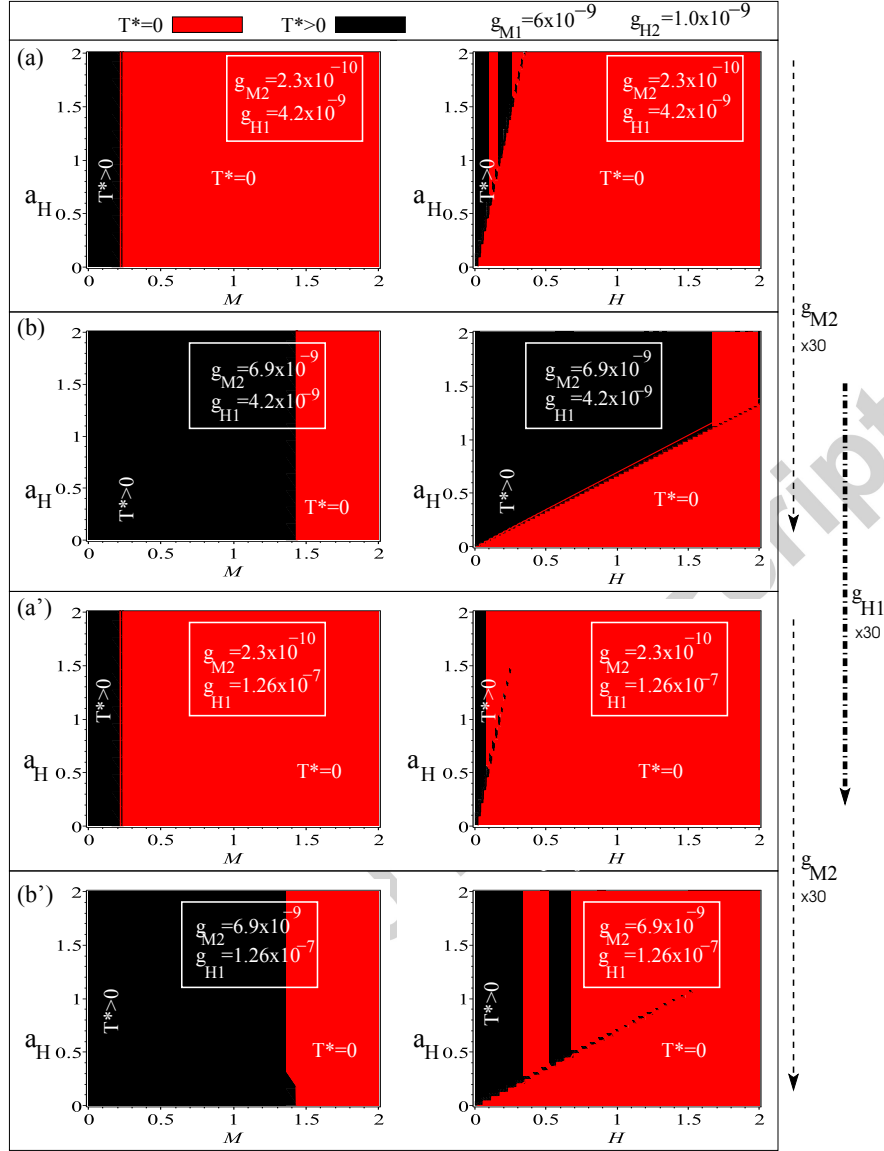


Figure 8: Parameter space where a tumour-immune coexistence steady state with $T^* > 0$ can exist. Here we show tumour size T^* vs. a_H vs. $M = M_1^*/M_2^*$ or $H = H_1^*/H_2^*$, as we vary g_{M_2} (increased 30-fold from 2.3×10^{-10} to 6.9×10^{-9}) and g_{H_1} (increased 30-fold from 4.2×10^{-9} to 1.26×10^{-7}): (a) $g_{M_2} = 2.3 \times 10^{-10}$, $g_{H_1} = 4.2 \times 10^{-9}$; (b) $g_{M_2} = 6.9 \times 10^{-9}$, $g_{H_1} = 4.2 \times 10^{-9}$; (a') $g_{M_2} = 2.3 \times 10^{-10}$, $g_{H_1} = 4.2 \times 30 \times 10^{-9} = 1.26 \times 10^{-7}$; (b') $g_{M_2} = 6.9 \times 10^{-9}$, $g_{H_1} = 4.2 \times 30 \times 10^{-9} = 1.26 \times 10^{-7}$. Here we chose $g_{H_2} = 1 \times 10^{-9}$, $g_{M_1} = 6 \times 10^{-9}$, $a_{H_2} = 0.001$ and vary a_{H_1} in the ratio $a_H = a_{H_1}/a_{H_2}$. The rest of parameter values are as in Table A.1.

279
280

emphasise here that small changes in g_{H_2} do not have a significant effect on tumour growth (also supported by the sensitivity analysis in Figure 14). To observe a difference between the

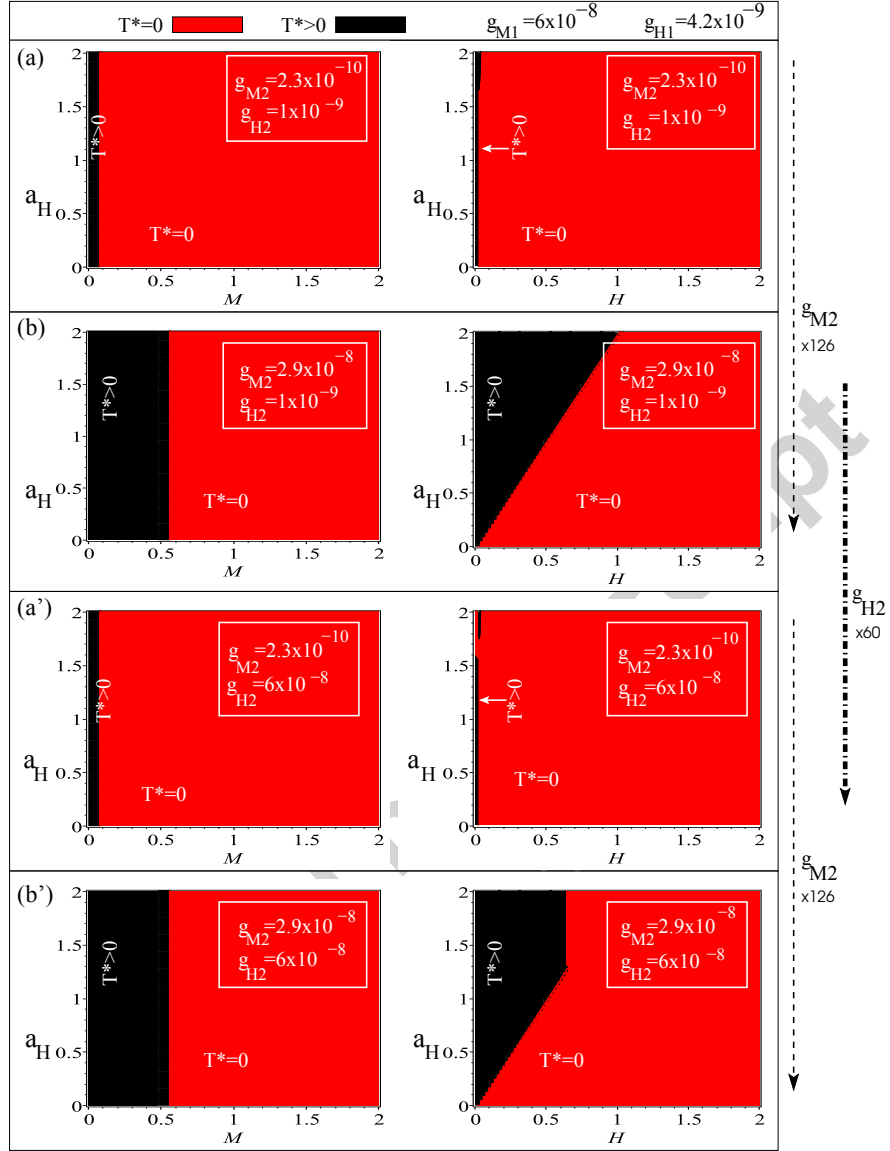


Figure 9: Parameter space where a tumour-immune coexistence steady state with $T^* > 0$ can exist. Here we show tumour size T^* vs. a_H vs. $M = M_1^*/M_2^*$ or $H = H_1^*/H_2^*$, for $g_{M1} = 6 \times 10^{-8}$ and different parameter values for g_{M2} (increased 126-fold from 2.3×10^{-10} to 2.9×10^{-8}) and g_{H2} (increased 60-fold from 1×10^{-9} to 6×10^{-8}): (a) $g_{M2} = 2.3 \times 10^{-10}$, $g_{H2} = 10^{-9}$; (b) $g_{M2} = 2.9 \times 10^{-8}$, $g_{H2} = 10^{-9}$; (a') $g_{M2} = 2.3 \times 10^{-10}$, $g_{H2} = 6 \times 10^{-8}$; (b') $g_{M2} = 2.9 \times 10^{-8}$, $g_{H2} = 6 \times 10^{-8}$. Here we chose $g_{H1} = 4.2 \times 10^{-9}$, $a_{H2} = 0.001$ and vary a_{H1} in the ratio $a_H = a_{H1}/a_{H2}$. The rest of parameter values are as in Table A.1.

281
282

diagrams in panels (a),(b) and those in panels (a'),(b') we had to increase g_{H2} by more than 40-fold (shown in panels (a'),(b') is the effect of a 60-fold increase in g_{H2}). In this case, the

283 increase in g_{H_2} affected mainly the region where $H = H_1^*/H_2^* > 1$ (see the right figures in
 284 panels (b),(b')).
 285 Overall, Figures 8 and 9 suggest that the parameters most likely to impact tumour growth/decay
 286 are g_{H_1} , g_{M_2} and g_{M_1} . We will return to this aspect in Section 3.3, when we will perform a
 287 sensitivity analysis for the transient dynamics of model (3).

288 3.2. Short-term and long-term dynamics

289 To investigate numerically the long-term dynamics of immune cells and cancer cells, we use
 290 the parameter values described in Table A.1. We chose to use the same parameter values as
 291 in Section 2.2, to investigate the effect of introducing a tumour on the interactions between Th
 292 cells and macrophages. The initial values for our simulations are: $T(0) = 10^5$, $M_1(0) = 100$,
 293 $M_2(0) = 0$, $H_1(0) = 0$ and $H_2(0) = 0$. As before, we chose $M_1(0) > 0$ since the M1 macrophages
 294 are the primary host defence [33].

295 *Tumour elimination.* First, we focus on the parameter ranges for r_{M_1} and r_{M_2} that ensure tu-
 296 mour elimination in the presence of a type-I immune response, a type-II immune response, or a
 297 combination of both type-I/type-II immune responses. In this case, the dynamics will approach
 298 the stable steady state $(0, H_1^*, H_2^*, M_1^*, M_2^*)$, and the dominant immune responses are consistent
 299 with those in the bifurcation diagram shown in Figure 5. We emphasise this aspect by discussing
 300 separately the following two cases involving the activation rates a_{H_1}, a_{H_2} for the Th1 and Th2
 301 cells:

- 302 (1) *Case $a_{H_1} < a_{H_2}$.* Figure 10 illustrates the short-term dynamics (panels (i); $t < 30$ days)
 303 and long-term dynamics (panels (ii); $t \leq 100$ days) of model (3), for two different cases:
 304 (a) $r_{M_1}/r_{M_2} = 1.8 \gg 1$, and (b) $r_{M_1}/r_{M_2} = 0.625$. In panel (a)(i) we observe a double
 305 switch between the M1 and M2 cells that dominate the dynamics (and this is associated
 306 with only one switch in the Th1-Th2 dynamics). In panel (b)(i) we observe a single switch
 307 the dynamics of both M1 and M2 cells, and Th1 and Th2 cells. In all cases the tumour is
 308 eliminated, and the results are consistent with the bifurcation diagrams in Figure 5(a).
 309 (2) *Case $a_{H_1} > a_{H_2}$.* Figure 11 illustrates the short-term dynamics (panels (i)) and long-term
 310 dynamics (panels (ii)) of model (3) for two cases: (a) $r_{M_1}/r_{M_2} = 1.8$, (b) $r_{M_1}/r_{M_2} = 0.625$.
 311 In panel (a)(i) we observe a double switch between the M1 and M2 cells that dominate
 312 the dynamics (but this is not associated with any switch in the Th1-Th2 dynamics). In panel
 313 (b)(i) we observe a double switch between the Th1 and Th2 cells that dominate the dynamics
 314 (associated with a single switch in the M1-M2 dynamics).

315 *Tumour persistence.* Figure 12(a) shows tumour growth for $r_{M_1}/r_{M_2} = 1$ (and $g_{H_1} = 4.2 \times 10^{-9}$,
 316 $g_{M_2} = 7.3 \times 10^{-10}$). In the long term, the dynamics of system (3) approaches the stable steady
 317 state $(T^*, H_1^*, H_2^*, M_1^*, M_2^*)$. By investigating the short-term dynamics of model (3) (see panel a(i))
 318 we observe a switch in both the Th1-Th2 and M1-M2 dynamics, from an initial type-I response
 319 to a later type-II response. This is consistent with the bifurcation results in Figure 8(b), where
 320 tumour exists for $M, H \ll 1$ (where $M = M_1^*/M_2^*$, $H = H_1^*/H_2^*$). Moreover, we would like
 321 to emphasise that the dormant behaviour exhibited by the tumour for $t \in (5, 15)$ is mainly the
 322 result of a very large M1 population that keeps the tumour under control. As soon as this M1
 323 population is reduced, the tumour grows fast towards its carrying capacity.

324 The difference between tumour dormancy/growth in Figure 12 and tumour elimination in
 325 Figures 10–11 is the result of (a) a small change in the rate at which tumour cells are eliminated

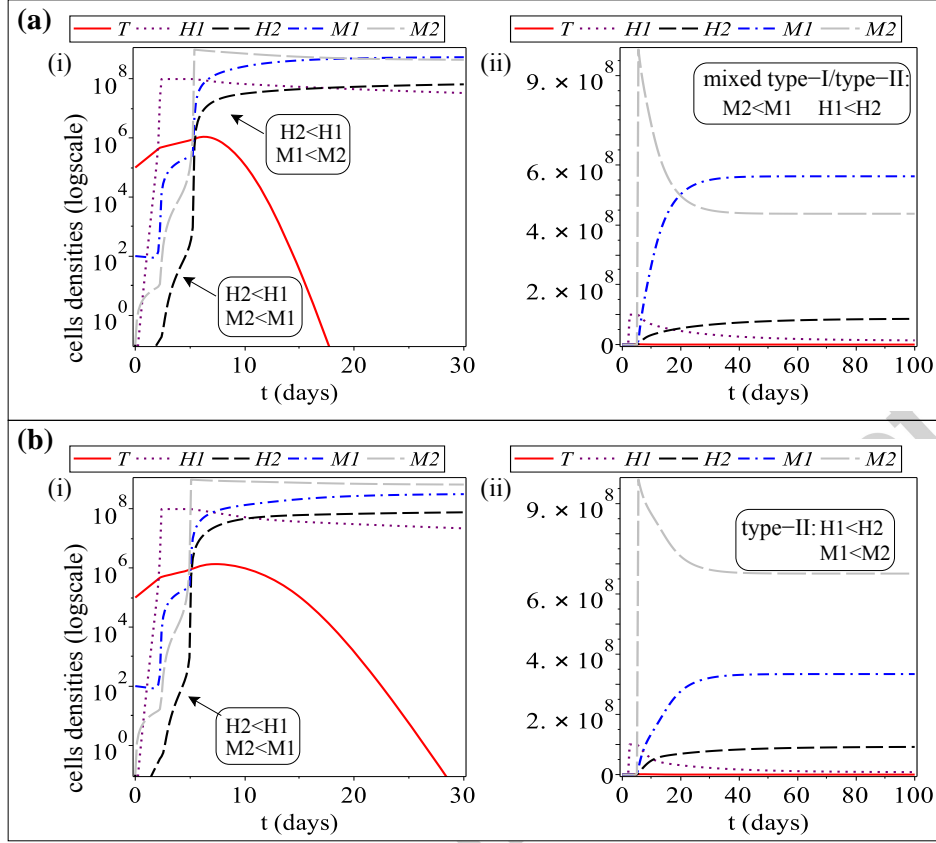


Figure 10: Dynamics of model (3), when $a_{H_1} = 0.001 < a_{H_2} = 0.008$ and the tumour is eliminated. For this case, we always have $H_1^* < H_2^*$. (a) Short-term dynamics (panel (i)) and long term dynamics (panel (ii)) when $r_{M_1} = 0.09$, $r_{M_2} = 0.05$. (b) Short-term dynamics (panel (i)) and long-term dynamics (panel (ii)) for $r_{M_1} = 0.05$, $r_{M_2} = 0.08$. For these simulations we also choose: $g_{H_1} = 4.8 \times 10^{-9}$, $g_{M_2} = 2.3 \times 10^{-10}$, $\alpha = 0.69$. For the rest parameters values see Table A.1.

326 by the Th1 cells via the cytokines they produce (from $g_{H_1} = 4.4 \times 10^{-9}$ for tumour elimination to
 327 $g_{H_1} = 4.2 \times 10^{-9}$ for tumour growth), and (b) a small change in the rate at which M_2 macrophages
 328 can support tumour growth (from $g_{M_2} = 2.3 \times 10^{-10}$ for tumour elimination to $g_{M_2} = 7.3 \times 10^{-10}$
 329 for tumour growth). However, different other combinations of parameter changes can lead to
 330 similar tumour dormant behaviours (which seem to be controlled by relatively high levels of M1
 331 cells). To investigate the effect of small changes in parameter values on the level of tumour and
 332 immune cells during dormancy (not only M1 but also M2, Th1 and Th2 cells), in Section 3.3 we
 333 will perform a sensitivity analysis.

334 In Section 1 we mentioned the experimental results in [5] (see also Figure 2(c)), which
 335 showed tumour growth being associated with a shift in the ratio of M1 and M2 cells: from
 336 M1:M2 \approx 90:10 on day 7, to M1:M2 \approx 20:80 on day 14. To compare these experimental results
 337 with our numerical results, in Figure 12(b) we show the percentage of Th cells and macrophages
 338 on day 4.5 (when tumour is small), day 14 (when tumour is dormant) and day 19 (when tumour

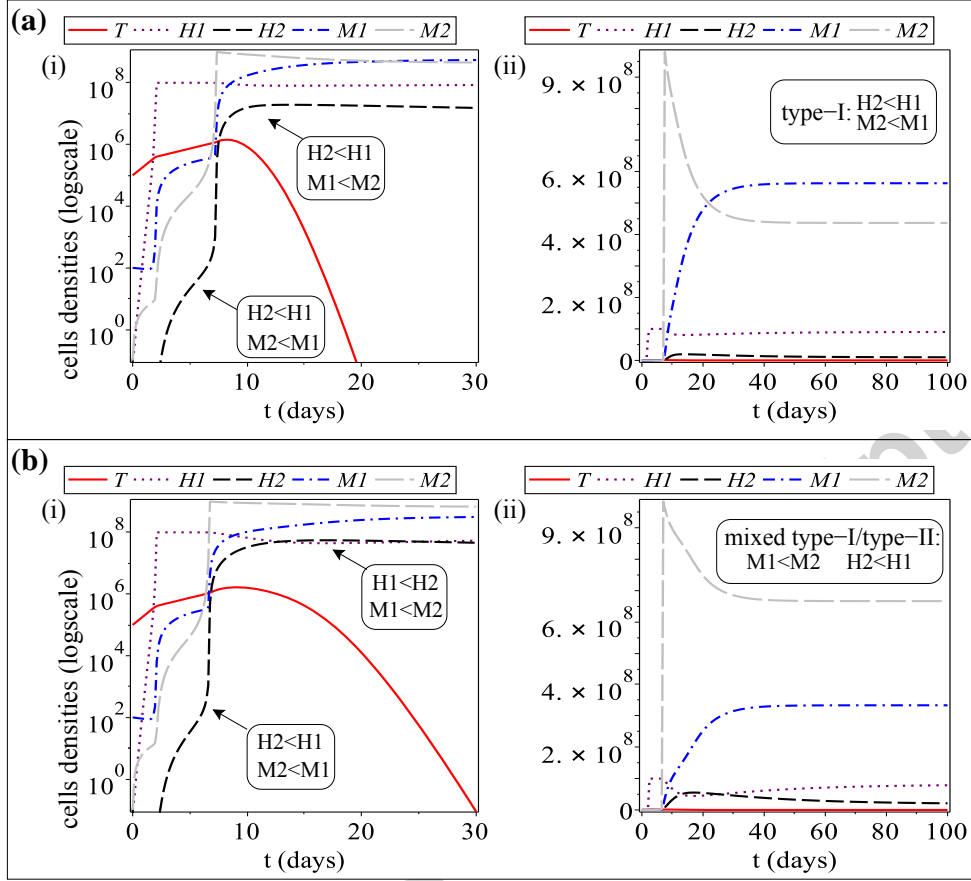


Figure 11: Dynamics of model (3) when $a_{H_1} = 0.008 > a_{H_2} = 0.001$ and the tumour is eliminated. For this case, we always have $H_1^* > H_2^*$. (a) Short-term dynamics (panel (i)) and long-term dynamics (panel (ii)) for $r_{M_1} = 0.09$, $r_{M_2} = 0.05$. (b) Short-term dynamics (panel (i)) and long-term dynamics (panel (ii)) for $r_{M_1} = 0.05$, $r_{M_2} = 0.08$. For these simulations we also choose $g_{H_1} = 4.8 \times 10^{-9}$, $g_{M_2} = 2.3 \times 10^{-10}$, $\alpha = 0.69$. For the rest of parameters values see Table A.1.

339 approaches its carrying capacity). We see that tumour growth is not only associated with an in-
 340 crease in the percentage of M2 cells (as shown experimentally in [5]), but also with an increase
 341 in the percentage of Th2 cells (as shown experimentally in [47]). Note that this is one possible
 342 outcome of the model. Changes in parameter values could lead to different ratios of Th2:Th1
 343 cells and M2:M1 cells as tumour progresses.

344 Finally, we recall that the results in Figure 8(b) suggested that by increasing g_{M_2} one could
 345 observe tumour existence also in the case of a type-I immune response with $M, H > 1$ (in addition
 346 to a type-II response, with $M, H < 1$). We show in Figure 13 the short-term and long-term
 347 dynamics of model (3), characterised by the persistence of tumour cells at lower values (with a
 348 maximum of about 5×10^7 cells). This persistence is the result of a type-I immune response,
 349 which alternates for short periods of time with a type-II response. We emphasise that these oscil-
 350 lations in tumour growth/decay (triggered by oscillations in the type-I/type-II immune responses)

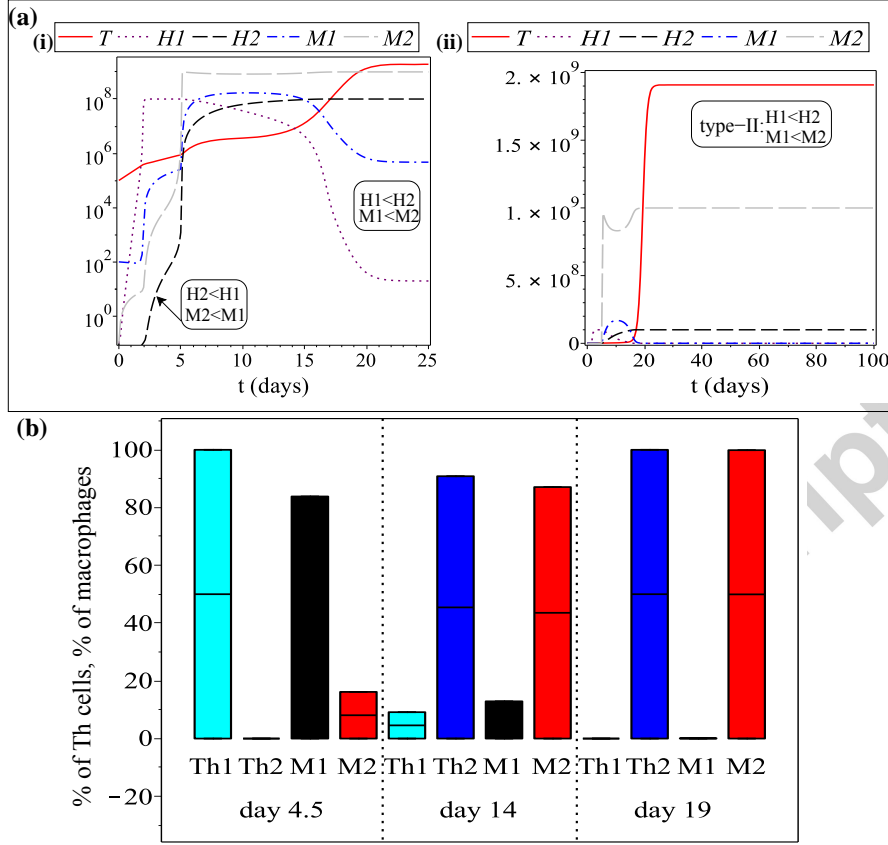


Figure 12: (a) Tumour growth exhibited by model (3), when $a_{H_1} = a_{H_2} = 0.008$ and $r_{M_1} = 0.09$, $r_{M_2} = 0.05$. Note that tumour growth is associated with a type-II immune response: $M_1^* < M_2^*$ and $H_1^* < H_2^*$. (i) short-term dynamics ($t < 25$; the y-axis is shown on a log-scale); (ii) long-term dynamics. Here we choose: $g_{H_1} = 4.2 \times 10^{-9}$, $g_{M_2} = 7.3 \times 10^{-10}$, $\alpha = 0.69$. For the rest of parameters values see Table A.1. (b) Percentage of Th cells and macrophages calculated on 3 different days ($t=4.5$, $t=14$, $t=19$), for the numerical simulations shown in (a).

351 might not be always observable in a clinical setting. [48] showed that in humans, the tumour di-
 352 agnostic level is between $10^7 - 10^9$ cells. Therefore, 5×10^7 cells might not be always detected
 353 clinically.

354 3.3. Sensitivity analysis

355 Since the majority of parameter values could not be approximated from the literature, in the
 356 following we perform a sensitivity analysis to investigate the effect of changes in these param-
 357 eters on the growth of the tumour. To this end, we vary each parameter P by $\pm 10\%$ or $\pm 90\%$ at a
 358 time (i.e., $P \pm \Delta P$, with $\Delta P = 0.1P$ or $\Delta P = 0.9P$), and investigate the impact of this change on
 359 tumour size on day 10 (an arbitrarily-chosen day, when the tumour has not reached its maximum
 360 size yet). The relative change in tumour size on day 10 (i.e., $\Delta T(10)$) is used in Figure 14 to plot

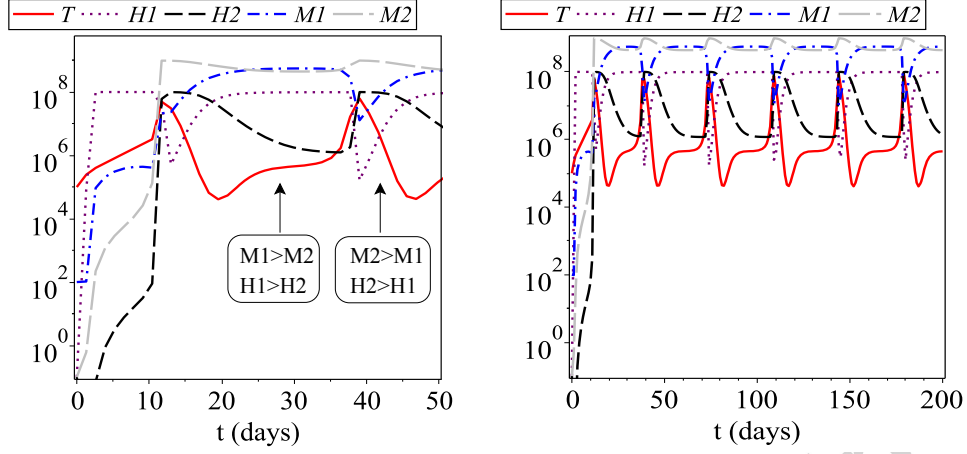


Figure 13: Short-term dynamics (panel (a)) and long-term dynamics (panel (b)) of model (3), when $g_{M_2} = 7.3 \times 10^{-9}$, $g_{H_2} = 8.546835 \times 10^{-9}$, $a_{H_1} = 0.08 \gg a_{H_2} = 0.001$, $r_1 = 0.09 \gg r_2 = 0.005$. For the rest parameters values see Table A.1. In this case, the tumour persists being controlled alternatively by a type-I and a type-II immune response.

361 the ratio of relative changes: $(\frac{\Delta T(10)}{T(10)}) / (\frac{|\Delta P|}{|P|})$.

362 Figure 14 illustrates tumour sensitivity to changes in the parameter values: (a) by $\pm 10\%$ and
 363 (b) by $\pm 90\%$. The parameters that have the most significant effect on tumour size when varied
 364 by $\pm 10\%$ are: the tumour growth rate (α), the proliferation of Th1 cells (p_{H_1}), the elimination
 365 rate of tumour cells by the Th1 cells (g_{H_1}) and by M1 macrophages (g_{M_1}), the carrying capacity
 366 of Th cells (m_1), the carrying capacity of macrophages (m_2), the transition rate from M1 to M2
 367 cells (r_{M_1}), the activation rate of M1 cells (a_{M_1}) and the proliferation of M2 cells in the presence
 368 of type-II cytokines (p_{M_2}). It is likely that p_{M_1} might also have higher impact on tumour if we
 369 would consider higher self-proliferation rates for M1 cells. The parameters that have the most
 370 significant impact on tumour size when varied by $\pm 90\%$ are p_{H_1} and α (similar to case (a)). Also
 371 a decrease in m_1 , g_{H_1} , g_{M_1} and r_{M_1} leads to a significant increases in tumour size (see the inset
 372 in the right panel of Figure 14(b)). (Note that, in Figure 14(b) is difficult to see the reduction in
 373 tumour size as we vary the parameter values - because of the very large increases in tumour size.)
 374 We also need to emphasise that g_{H_2} and g_{M_2} (both associated with a type-II immune response)
 375 do not have a significant impact on tumour reduction. This is a particularly interesting result that
 376 might be of biological interest, since at least g_{H_2} has the same order of magnitude – see Table
 377 A.1 – as parameters g_{H_1} and g_{M_1} (which have a significant effect on tumour reduction/growth).
 378 Moreover, this result supports the idea that the elimination of tumour cells by the Th2 cells in
 379 Mattes et al. [2] was not the result of direct Th2-tumour interactions (via Th2-cytokines), but the
 380 combined effect of different anti-tumour cells.

381 To gain a better understanding on tumour dormancy (and on the role of immune response in
 382 controlling tumour growth), next we perform a tumour and immune sensitivity to small changes
 383 in four parameter values associated with anti-tumour/pro-tumour immune responses: g_{H_1} , g_{H_2} ,
 384 g_{M_1} , g_{M_2} . To this end, we start with the baseline parameters that lead to tumour dormancy/growth
 385 in Figure 12(a), and we vary them by $\pm 10\%$ to investigate the changes in tumour and immune
 386 sizes at day $t = 10$ (when dormancy occurs). First, we note that during tumour dormancy,

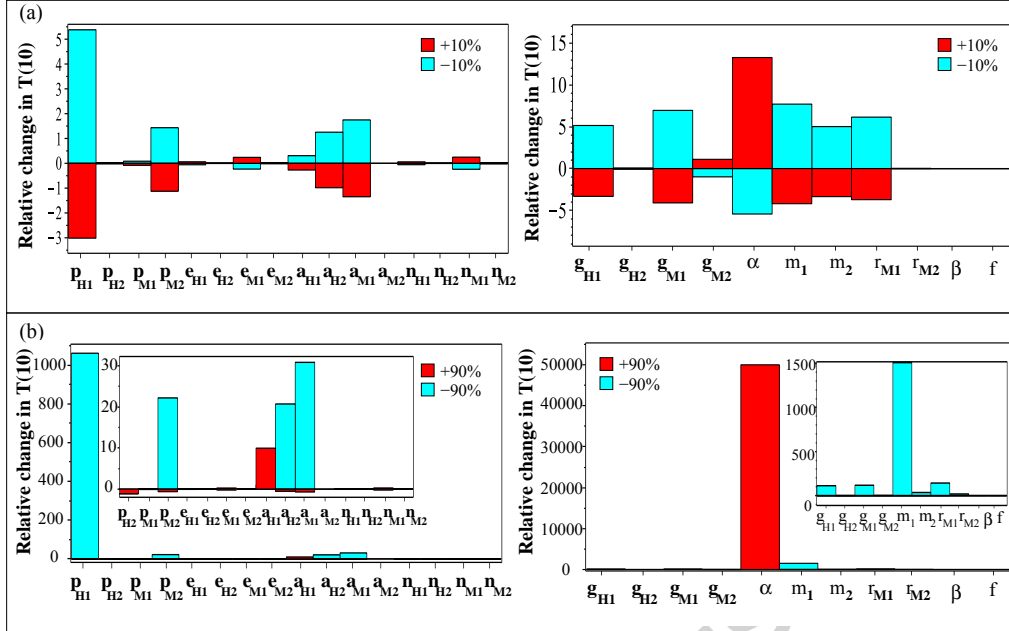


Figure 14: Sensitivity analysis for model (3), when each model parameter is increased (red bars) and decreased (cyan bars) by: (a) 10% and (b) 90%. Here, we show the relative changes in tumour size on day $t = 10$ in response to the changes in the parameter P values: $(\Delta T(10)/T(10))/(\Delta P/|P|)$, with the negative values showing the decrease in tumour size, and the positive values showing the increase in tumour size. The baseline parameters are those shown in Table A.1. The inset figures in panel (b) show the details of the sensitivity analysis for the parameters that do not lead to the two largest changes in tumour size (i.e., after we remove p_{H1} and α from the bar plots).

387 changes in parameter g_{H1} have a slightly bigger impact on tumour at day $t = 10$ ($T(10)$) compared
 388 to changes in parameter g_{M1} - see Fig. 15(a). This is in contrast to the case of tumour elimination
 389 (see Fig. 14(a), left panel) where g_{M1} has a bigger impact on $T(10)$ compared to g_{H1} . Second,
 390 we note that during tumour dormancy g_{M2} has a stronger impact on $T(10)$ (see Fig. 15(a))
 391 compared to the case of tumour elimination where g_{M2} barely affects $T(10)$ (see Fig. 14(a)). In
 392 fact, we observe that $\pm 10\%$ changes in the three parameters g_{H1} , g_{M1} and g_{M2} , lead to changes
 393 of relatively similar magnitudes in tumour cells (Fig. 15(a)), and in each of the four types of
 394 immune cells (Figs. 15(b)-(d)). This suggest that tumour dormancy is the result of a delicate
 395 balance between the anti-tumour effect of Th1 and M1 cells, and the pro-tumour effect of M2
 396 cells. Moreover, by looking at panels (b)-(e) we observe that the effects of g_{M1} and g_{M2} do not
 397 balance perfectly during dormancy: g_{M2} causes slightly larger effects in both tumour and immune
 398 responses compared to g_{M1} (and this imbalance eventually translates into tumour relapse).

399 To conclude the discussion on the effects of parameters g_{H1} , g_{M1} and g_{M2} on the immune
 400 responses during tumour dormancy, we stress that while it was expected that an increase in g_{M1}
 401 and g_{H1} would be associated with an increase in $M1$ and $H1$ (through the direct reduction of
 402 tumour), it was however unexpected that g_{H1} would have an effect on $H2$ and $M2$ cells (stronger
 403 than the effects of parameters g_{H2} and g_{M2}).

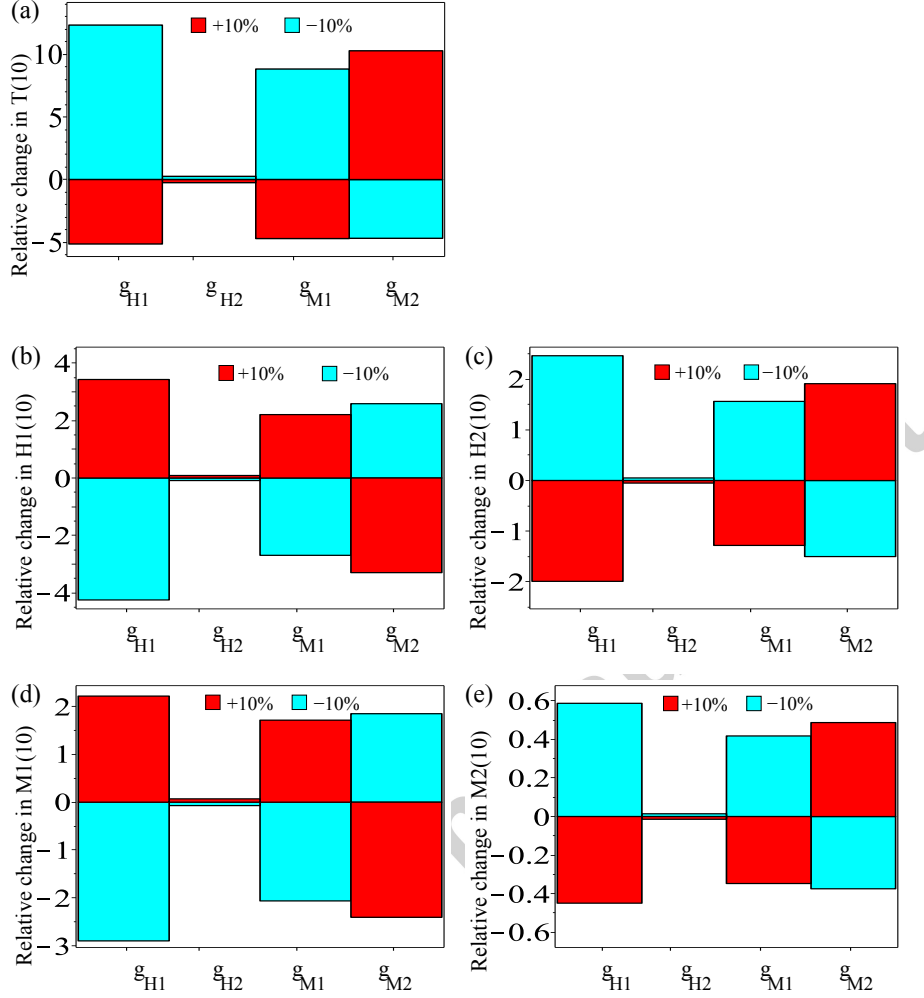


Figure 15: Sensitivity analysis of the tumour and immune responses for model (3), during tumour dormancy. We focus on four model parameters (g_{H1} , g_{H2} , g_{M1} , g_{M2}), and increase them (red bars) and decrease them (cyan bars) by 10%. We also show the relative changes in tumour size and all four immune cells on day $t = 10$ in response to the changes in the parameter P values: $(\Delta M_i(10)/M_i(10))/(|\Delta P|/|P|)$ and $(\Delta H_i(10)/H_i(10))/(|\Delta P|/|P|)$, for $i = 1, 2$: (a) Relative change in $T(10)$; (b) Relative change in $H_1(10)$; (c) Relative change in $H_2(10)$; (d) Relative change in $M_1(10)$; (e) Relative change in $M_2(10)$. The baseline parameters are those shown in the caption of Fig. 12.

404 4. Summary and Discussion

405 In this article, we derived two mathematical models for the dynamics of immune responses
 406 involving Th1&Th2 and M1&M2 cells, in the absence and in the presence of tumour cells. We
 407 then used these models to propose mechanistic hypotheses that could explain the contradictory
 408 results in the experimental data for the immune response against melanoma B16 cells.

409 We started with a model that considered only the interplay between M1 and M2 macrophages,

410 and Th1 and Th2 cells in response to some external pathogen that first triggered an M1 response
 411 (i.e., $M_1(0) > 0$). To shed light on the complexity of model dynamics, we first calculated the
 412 steady states (to study the long-term behaviour of the model) and then we performed numerical
 413 simulations for the short-term and long-term model dynamics. By focusing on the ratio r_{M_1}/r_{M_2}
 414 (of macrophages re-polarisation rates), and the activation rates of Th cells (a_{H_1} , a_{H_2}) in the
 415 presence of signals received from macrophages, we were able to classify the immune responses
 416 into: a type-I dominated response ($H_1 > H_2$, $M_1 > M_2$), a type-II dominated response ($H_1 < H_2$,
 417 $M_1 < M_2$), or a combination of type-I and type-II responses (e.g., $M_1 > M_2$ but $H_1 < H_2$);
 418 see the results in Figs. 6, 7. Note that experimental studies have shown that different diseases
 419 associated with the Th1 and Th2 immune responses can show different levels of M1 and M2
 420 macrophages. For example, in [49] (Table 1), the authors showed that about 60.7% of Th1
 421 disease cases investigated (in the context of infectious mononucleosis and Crohn's disease) have
 422 $M_1 > M_2$, and about 72.5% of Th2 disease cases investigated (in the context of allergic nasal
 423 polyps, oxyuriasis, wound healing and foreign body granulomas) have $M_2 > M_1$. Thus their
 424 results suggest that there are Th1 diseases with a higher level of M2 cells, and Th2 diseases with
 425 a higher level of M1 cells (consistent with our numerical results).

426 Next, we generalised the mathematical model to consider also tumour dynamics. We showed
 427 numerically that tumour elimination can occur both in the presence of a type-I dominated im-
 428 mune response, as well as in the presence of a type-II dominated response (as observed exper-
 429 imentally in [2, 3, 4]; see also Figures 1, 2). We need to emphasise that tumour elimination
 430 also required a relatively large tumour lysis rates g_{H_1} and g_{M_1} and a low g_{M_2} . As before, the
 431 type of immune response that dominated the dynamics was decided by the ratio r_{M_1}/r_{M_2} and the
 432 activation level of immune cells (a_{H_1} , a_{H_2}).

433 Tumour growth towards carrying capacity (or some very large size) was always associated in
 434 our study with a long-term type-II immune response, i.e., $H_2 > H_1$, $M_2 > M_1$; see Figure 12.
 435 In this case, the initial type-I response (with $M_1 > M_2$ for $t \leq 5$ days and $H_1 > H_2$ for $t \leq 10$
 436 days) was always replaced in the long-term by a type-II immune response. This shift from a
 437 type-I to a type-II response was observed also experimentally in the context of cancer growth.
 438 For example, Chen et al. [5] showed a 90:10 ratio of M1:M2 macrophages in B16F10 melanoma
 439 tumours around day 7, and a 20:80 ratio of M1:M2 macrophages around day 14 (see Figure 2(c)).
 440 Other experimental studies have described a shift from a Th1 response to a Th2 response during
 441 the first 14-20 days of progression of malignant tumours (see [50] for human melanoma). These
 442 experimental studies also suggested that one could improve cancer outcome by re-polarising the
 443 macrophages and Th cells from a type-II response associated with tumour growth to a type-I
 444 response associated with tumour decay [51]. Our theoretical results are in agreement with the
 445 experimental suggestion that a type-I response improves long-term cancer outcome. Moreover,
 446 our results also emphasise the complexity of the tumour-immune system, in which a type-I im-
 447 mune response might alternate with a type-II immune response (for short-term or long-term),
 448 thus leading only to tumour control but not tumour elimination.

449 We stress that the interaction between the pro-tumour/anti-tumour effects of macrophages
 450 and Th cells affects tumour dynamics in a nonlinear manner. For example, a 10-fold increase
 451 in the rate of tumour clearance by M1 macrophages (g_{M_1}) caused tumour persistence only in
 452 the presence of a type-II immune response (i.e., a type-I immune response would be associated
 453 to tumour clearance). To ensure tumour persistence also in the presence of a type-I response,
 454 the 10-fold increase in g_{M_1} needed to be counter-balanced by at least a 150-fold increase in the
 455 tumour growth rate in the presence of M2 cells, g_{M_2} (see Figures 8 and 9). This nonlinearity in
 456 the anti-tumour response is likely the result of the interplay between the macrophages and the

457 Th cells, an aspect not very well studied at experimental level. Although there are some studies
 458 on the interactions between macrophages and $CD4^+$ T cells, for example, in the context of breast
 459 and lung cancer [52, 53], or in the context of rheumatoid arthritis [54], such studies do not shed
 460 much light on the nonlinear interactions between these different types of immune cells.

461 In the context of the anti-tumour effect of macrophages, the sensitivity analysis in Figure
 462 14(a) suggested that tumour elimination was mainly the effect of M1 macrophages (and to a
 463 lesser extent the effect of Th1 cells). This is an interesting hypothesis generated by the model,
 464 which, if validated experimentally, could influence the current anti-tumour immune therapies
 465 that focus mainly on T cell responses [55, 56]. In contrast, the sensitivity analysis in Figure
 466 15 suggested that the transient decrease in tumour size on day 10 during tumour dormancy was
 467 mainly the effect of Th1 cells (and to a lesser extent the effect of M1 cells). In fact, the tumour
 468 dormant behaviour was the result of a delicate balance between the anti-tumour responses of Th1
 469 and M1 cells, and the pro-tumour responses of M2 cells. In addition, the results in Figures 8 and
 470 9 suggested that the three parameters, g_{H_1} , g_{M_1} and g_{M_2} , influenced also the asymptotic behaviour
 471 of model (3). This is in support of the idea that anti-cancer immunotherapies should focus on the
 472 combined effect of T cells and M1 macrophages.

473 The results in Figure 8 suggested that there could be very few M2 cells (and many M1 and
 474 Th1 cells), but if these M2 cells secrete large amounts of type-II cytokines (i.e., large g_{M_2}),
 475 they can skew the tumour microenvironment in favour of tumour sustenance and growth. This
 476 would support the experimental results in Mattes et al. [2], where a type-I environment was not
 477 enough to eliminate B16F10 melanoma cells. The authors in [2] recognised that the inability
 478 of Th1 cells to eradicate tumours might have been influenced by the presence of pro-angiogenic
 479 tumour-infiltrating macrophages (i.e., M2 cells), but they did not measure the levels of M2 and
 480 M1 macrophages, nor the levels of Th1 and Th2 cells. In fact, Mattes et al. [2] identified the
 481 Th1 and Th2 immune responses by the levels of type-I and type-II cytokines produced by these
 482 cells: high IL-5, IL-13 and IL-4 for a Th2-dominated response, and high IFN- γ , TNF- α and IL-
 483 13 for a Th1-dominated response (note here the relatively high levels of IL-13 observed during
 484 both Th1 and Th2 responses; and the fact that IL-13 is also involved in the alternative activation
 485 of M2 macrophages [57]). Since many experimental studies focus on the levels of cytokines as
 486 a proxy for the number of immune cells corresponding to a type-I or type-II response [2, 53],
 487 to be able to test our hypothesis regarding the role of g_{H_2} and M2 cells on tumour persistence
 488 during type-I responses, we need to extend model (3) by incorporating explicitly the effects of
 489 type-I and type-II cytokines on tumour-immune interactions (i.e., an approach similar to [17],
 490 where a mathematical models incorporated the effects of type-I, type-II, tumour-promoting and
 491 tumour-suppressing cytokines).

492 In this study, to keep the models relatively simple, we ignored deliberately the microenviron-
 493 ment which can alter the immune response against cancer [58]. However, the incorporation of the
 494 explicit effects of type-I and type-II cytokines (which can be further altered by the tumour cells
 495 [59]) would allow us not only to compare our results with available experimental cytokine data,
 496 but also to gain a better understanding of how to control cell-cell communication (by controlling
 497 cytokine signalling) with the ultimate goal of improving cancer immunotherapies.

498 Note from Table A.1 that models (1) and (3) contain both fast and slow variables. One could
 499 have used a quasi-steady state analysis to simplify the models. However, such an analysis might
 500 lead to limitations in our understanding of the transient dynamics of the Th1-Th2 and M1-M2
 501 cells (see, for example the study in [60]). This type of transient dynamics was observed in ex-
 502 perimental studies on early tumour behaviours, which suggested that the ratios of Th1/Th2 cells
 503 or M1/M2 cells can be used as independent predictive markers of patient survival [61, 47, 5].

504 In this theoretical study we showed that these ratios of immune cells can change once or twice
 505 before they stabilise towards a steady state (and they stabilise when the tumour reaches either
 506 a very large size or is eliminated; see Figures 10 – 12). The changes in the dominating Th or
 507 macrophages dynamics are not always correlated with each other. Moreover, we showed the
 508 possibility of having a long-term oscillatory tumour-immune dynamics characterised by low tu-
 509 mour values and periodic changes between type-I and type-II immune responses; see Figure 13.
 510 While sustained periodic tumour oscillations are not very often observed in clinical studies (al-
 511 though see [62]), we emphasise that model (3) exhibits such oscillations for tumour sizes around
 512 the detection threshold (of about $10^7 - 10^8$ cells [48]). This suggest that oscillations between
 513 type-I and type-II immune responses (in the presence of tumour) might be more common in clinical/
 514 experimental settings but they might not be measured since the tumour cannot be detected.
 515 Overall, we hypothesise that trying to predict the long-term outcome of the tumour while the
 516 ratios Th1/Th2 and M1/M2 are still varying due to the cross-talk with the tumour environment,
 517 might not always offer accurate predictions on patient survival.

518 At a more theoretical level, it would be interesting to investigate the differences between
 519 the double feedback in tumour-immune dynamics modelled in this study, and a single feedback
 520 for tumour-immune interactions. Such an investigation (to be the subject of a future study)
 521 would allow us to uncover the minimal biological mechanisms that need to be incorporated into
 522 a model to explain the dominant type-I and/or type-II immune responses associated with cancer
 523 immunotherapies.

524 Finally, these numerical results for systems (1) and (3) have generated two new mathematical
 525 questions that will be answered analytically in future studies: (i) analytical investigation of fast
 526 and slow parameters that control transient and long-term tumour-immune behaviours, and how
 527 the simplified dynamics in the slow/fast models matches the original dynamics; (ii) analytical
 528 investigation of the Hopf bifurcation that generated the limit cycle shown in Figure 13.

529 *Biological realism of the parameter values and overall results.* The results of this study depend
 530 on the parameter values described in Table A.1. Some of these values were taken from the literature,
 531 others were approximated based on published experimental results, and the remaining
 532 values were varied within some estimated ranges (see Appendix A). This approach is very
 533 common in the mathematical immunology literature, due to a lack of quantitative results regarding
 534 the immune responses following various antigen stimulations. In addition to the fact that
 535 very few labs measure and estimate kinetic parameters (the majority of such studies focusing on
 536 lymphocyte kinetics following pathogen stimulation [63, 64, 65]), there is also the difficulty of
 537 interpreting kinetic data; see the review in [65]. Moreover, the few rigorously estimated kinetic
 538 parameters in the mathematical immunology literature depend on the estimation method used, as
 539 emphasised in [66]. A more detailed discussion on model validation and parameter estimation in
 540 mathematical immunology can be found in [67].

541 Based on these facts, we acknowledge that the majority of models in the mathematical immunology
 542 literature, including this particular study, can have at this moment only a theoretical
 543 value. In particular, the model presented here can only propose hypotheses regarding the possible
 544 outcomes of the interactions between the Th1-Th2 and M1-M2 immune responses, in the
 545 absence/presence of tumour cells.

546 We showed that small variations in the values of parameters that control tumour cells lysis
 547 via anti-tumour cytokines (e.g., g_{H_1} , g_{M_1} , g_{M_2}), or the parameters for the activation of Th
 548 cells (a_{H_1} , a_{H_2}), or the macrophages re-polarisation rates (r_{M_1} , r_{M_2}) could explain the variety of
 549 tumour-immune dynamics observed in the experimental literature. To obtain a better understand-

ing of immune responses to specific diseases, the next step would be to quantify the rates that control various type-I and type-II immune responses. Therefore, for a better mechanistic understanding of the *in vivo* immune responses, which can be obtained with a more realistic *in silico* model, mathematicians (and immunologists) need to have access to relevant experimental data that could then be used to parametrise the mathematical models. The goal of our present study was not to parametrise the models to specific diseases, but to propose some general hypotheses regarding the processes involved in different immune responses.

Acknowledgements

RE acknowledges partial support from an Engineering and Physical Sciences Research Council (UK) First Grant number EP/K033689/1, and from a Northern Research Partnership (Scotland) grant.

Appendix A. Parameter values

In Table A.1 we summarise the parameter values used throughout this theoretical study. Some of these values were taken directly from existent mathematical literature, while other values were approximated based on experimental studies (marked by “*” in Table A.1); see also the discussion below. However, there were a few parameters for which we could not find any values, so we had to provide estimates for them. Some of these estimates were varied within specified ranges (see Table A.1).

Next, we discuss the parameter values we approximated using experimental studies, and the values taken from the literature (especially if different mathematical studies used different parameter values).

- Danciu et al. [68] have shown that melanoma cells have a doubling time between 17.2 hours and 24 hours, which corresponds to a tumour growth rate of 0.69 – 0.97. For simplicity, throughout this study we choose $\alpha = 0.69/\text{day}$.
- The proliferation of Th1 and Th2 cells occurs in the presence of type-1 and type-2 cytokines produced by the cells themselves and by the macrophages in the environment. For simplicity (and since we could not find data on the interactions between cytokines and cells; i.e., interaction radii, concentration of molecules that lead to cell proliferation), we assume that: (i) the concentrations of type-1 and type-2 cytokines are directly proportional to the density of M1 and M2 cells, and (ii) the interaction rates between cells and cytokines, p_{H_1} and p_{H_2} , are the same for both populations. This assumption is consistent with the approach in [18, 17], which consider similar recruitment rates for the Th1 and Th2 cells, in response to the cytokine environment. Due to a lack of consistent data on the growth of Th1 and Th2 populations (e.g., [17] assumed a growth rate of 0.09, while [18] assumed a growth rate between $10^2 - 10^4$), in this study, we used an estimated interaction rate of $p_{H_1} = p_{H_2} = 0.09$. Note that in Figure 14 we performed a sensitivity analysis of model dynamics to changes in parameter values, and investigated also the effect of variations in p_{H_1} and p_{H_2} .
- In regard to macrophages apoptosis rate, [7] used a death rate of 0.02/day. On the other hand [19] used a death rate of 0.2/day. However, experimental studies in [29] showed that

590 mice macrophages were cleared within 5-8 days of induction of inflammation, during the
 591 resolution stage of inflammation. However, since inflammation is a critical component
 592 of tumour progression [69], and we could not find any specific references regarding the
 593 half-life of macrophages inside tumours, we assumed here that the death rate of tumour
 594 macrophages is much lower than in [19], and more similar to the value in [7]: $e_{M_1} = e_{M_2} =$
 595 $0.02/\text{day}$.

- 596 • In regard to the proliferation of macrophages, [31] showed that by treating M2 macrophages
 597 with $5\mu\text{g}$ of IL-4 and $25\mu\text{g}$ anti-IL-4 antibody (to extend the half-life of the cytokine),
 598 it leads to an increased proliferation of macrophages 4 days later (from 1×10^6 in the
 599 control case to about 4.2×10^6 in the IL-4 case). We can approximate the interaction
 600 rate between M2 macrophages and the IL-4 cytokine concentration (produced by Th2
 601 cells) as $p_{M_2} = \ln(4.2)/(4 \times 30\mu\text{g}) = 0.012$. Assuming only $5\mu\text{g}$ of IL-4, it leads to
 602 $p_{M_2} = \ln(4.2)/(4 \times 5\mu\text{g}) = 0.072$. Throughout this study we consider an average of
 603 $p_{M_2} = 0.02$ (obtained assuming $17.5\mu\text{g}$ of IL-4 in the system). For the self-proliferation
 604 rate of M1 macrophages, we could not find any data. For for simplicity, throughout the
 605 simulations we used an average value $p_{M_1} = 0.02$. Nevertheless, in Figure 14 we also in-
 606 vestigated the sensitivity of tumour growth in response to changing $p_{M_1} \in (0.002, 0.038)$.
- 607 • In [70] it was suggested that a conservative estimate for the total number of macrophages
 608 in a normal adult mouse would be greater than 1×10^8 . Therefore, we have chosen the
 609 macrophages carrying capacity to be $m_2 = 10^9$.
- 610 • In the mathematical literature there are various estimations for tumour natural death rate.
 611 For example, [71] estimated a value of $2.08 \times 10^{-6}/\text{day}$, while [72] used arbitrary units and
 612 estimated tumour death rate at 0.1. On the other hand, [73] considered a tumour cell death
 613 rate within the range $(0,0.8)/\text{day}$. Since apoptosis is inactivated in cancer cells [74], in this
 614 study, we use an estimated value of natural death rate for cancer cells of $f = 10^{-8}/\text{day}$.
- 615 • In regard to the tumour killing rates by Th1 and Th2 cells (via the cytokines they produce),
 616 we note that [75] incubated 10^6 B16 melanoma cells with CD4 T cells. The maximum
 617 tumour lysis was 30%, obtained at an effector:target ratio of about 32:1. This corresponds
 618 to a tumour killing rate of $g_{H_1}, g_{H_2} = 5.3 \times 10^{-8}$ [22]. Throughout this study, we investigate
 619 what happens with the dynamics of model (3) when we vary $g_{H_1}, g_{H_2} \in (10^{-9}, 10^{-7})$.
- 620 • Various mathematical studies that investigated macrophages dynamics considered an ac-
 621 tivation rate within the range $(0.0-1.0)/\text{day}$, depending on the concentration of type-I and
 622 type-II cytokines that trigger their activation [76, 19]. However, the activation of M1
 623 macrophages is reduced in the presence of type-II cytokines such as IL-10 [76], and the
 624 activation of M2 macrophages is reduced in the presence of type-I cytokines such as
 625 IFN- γ [19]. Since the tumour environment contains both type-I and type-II cytokines,
 626 throughout this study we consider lower estimates for the macrophages activation rates:
 627 $a_{M_1}, a_{M_2} = 0.001$.

Param.	Description	Value	Units	Ref
α	tumour growth rate	0.69 – 0.97	1/day	*[68]
β	carrying capacity of the tumour	10^9	cell	[17, 77]
f	tumour natural death rate	10^{-8}	1/day	Estimate
g_{H_1}	killing rate of tumour cells by the Th1 cells	5×10^{-9} - 10^{-7}	1/day	Estimate
g_{H_2}	killing rate of tumour cells by the Th2 cells	10^{-9} ($10^{-9} - 10^{-7}$)	1/day	Estimate
g_{M_1}	killing rate of tumour cells by M1 macrophages	6×10^{-9}	1/((cell)(day))	Estimate
g_{M_2}	tumour growth rate in the presence of M2 cells	2.3×10^{-10} , 7.3×10^{-10} ($10^{-10} - 7.3 \times 10^{-9}$)	1/((cell)(day))	Estimate
n_{H_1}	inactivation rate of Th1 cells by tumour cells	10^{-7}	1/((cell)(day))	[17]
n_{H_2}	inactivation rate of Th2 cells by tumour cells	10^{-7}	1/((cell)(day))	[17]
n_{M_1}	inactivation rate of M1 cells by tumour cells	10^{-7} ($10^{-7} - 7 \times 10^{-4}$)	1/((cell)(day))	Estimate
n_{M_2}	recruitment rate of M2 cells in the presence of tumour cells	10^{-7} ($10^{-10} - 10^{-7}$)	1/((cell)(day))	Estimate
a_{H_1}	activation rate of Th1 cells	0.001-0.008	1/day	Estimate
a_{H_2}	activation rate of Th2 cells	0.001-0.008	1/day	Estimate
a_{M_1}	activation rate of M1 cells	0.001 ($10^{-4} - 10^{-2}$)	1/day	Estimate
a_{M_2}	activation rate of M2 cells	0.001 ($10^{-4} - 10^{-2}$)	1/day	Estimate
m_1	carrying capacity of Th cells	10^8	1/cell	[17]
m_2	carrying capacity of macrophages	10^9	1/cell	*[70]
p_{H_1}	interaction rate between Th1 cells and type-1 cytokines produced by the M1 cells, which leads to the proliferation of Th1 cells	0.09 (0.009 – 0.17)	1/(day)(cell)	Estimate
p_{H_2}	interaction rate between Th2 cells and type-2 cytokines produced by the M2 cells, which leads to the proliferation of Th2 cells	0.09 (0.009 – 0.17)	1/(day)(cell)	Estimate
p_{M_1}	proliferation rate of M1 cells	0.02 ($10^{-3}, 10^{-1}$)	1/day	Estimate
p_{M_2}	interaction rate between M2 cells and the IL-4 cytokines produced by Th2 cells, which leads to M2 proliferation	0.02	1/(day)(cell)	*[31]
r_{M_1}	M1→M2 transition rate	0.05-0.09	1/day	[19]
r_{M_2}	M2→M1 transition rate	0.05-0.08	1/ day	[19]
e_{H_1}	death rate of the Th1 cells	0.03	1/day	[7]
e_{H_2}	death rate of the Th2 cells	0.03	1/day	[7]
e_{M_1}	death rate of the M1 cells	0.02	1/day	[7]
e_{M_2}	death rate of the M2 cells	0.02	1/day	[7]

Table A.1: Table summarising the parameters that appear in models (1) and (3), and their values used throughout the numerical simulations. References marked by “*” correspond to parameter values that were approximated based on experimental studies. Some of the elements in column “Value” show not only the specific values used for the simulations, but also the parameter ranges (in parentheses) over which we varied those parameters.

628 **Appendix B. Non-negative solutions**

629 Here, we show that system (3) has non-negative solutions. Since (3) is a generalisation of
630 (1), the results hold also for model (1).

631 To start, we assume that $T(0), H_1(0), H_2, M_1(0), M_2(0) \geq 0$. Note that if $T(0) = 0, M_1(0) = 0,$
632 $M_2(0) = 0, H_1(0) = 0, H_2(0) = 0$, then the system is at equilibrium and the only solution is the
633 trivial one.

634 Assume that it is possible to have negative solutions. Then there exists a time $t_0 < \infty$ defined
635 as

$$t_0 = \inf\{t > 0 \mid T(t) < 0, H_1(t) < 0, H_2(t) < 0, M_1(t) < 0, \text{ or } M_2(t) < 0\}. \quad (\text{B.1})$$

636 We have the following inequalities:

- 637 • From equation (3a):

$$\frac{dT}{dt} \geq -T(f + g_{H_1}H_1 + g_{H_2}H_2 + g_{M_1}M_1 - g_{M_2}M_2), \quad \text{for } t \leq t_0. \quad (\text{B.2})$$

638 Since $T(t_0) \geq 0$, there exists a non-negative solution $T(t) \geq T(t_0)e^{-\int (f+g_{H_1}H_1+g_{H_2}H_2+g_{M_1}M_1-g_{M_2}M_2)ds}$
639 ≥ 0 , for $t \in (t_0 - \epsilon_1, t_0 + \epsilon_1)$.

- 640 • From equation (3b):

$$\frac{dH_1}{dt} \geq -H_1(n_{H_1}T + e_{H_1}), \quad \text{for } t \leq t_0. \quad (\text{B.3})$$

641 Since $H_1(t_0) \geq 0$, there exists a non-negative solution $H_1(t) \geq H_1(t_0)e^{-\int (n_{H_1}T+e_{H_1})ds} \geq 0,$
642 for $t \in (t_0 - \epsilon_2, t_0 + \epsilon_2)$.

- 643 • From equation (3c):

$$\frac{dH_2}{dt} \geq -H_2(n_{H_2} + e_{H_2}), \quad \text{for } t \leq t_0. \quad (\text{B.4})$$

644 Since $H_2(t_0) \geq 0$, there exists a non-negative solution $H_2(t) \geq H_2(t_0)e^{-\int (n_{H_2}T+e_{H_2})ds} \geq 0,$
645 for $t \in (t_0 - \epsilon_3, t_0 + \epsilon_3)$.

- 646 • From equation (3d):

$$\frac{dM_1}{dt} \geq -M_1(n_{M_1}T + e_{M_1} + r_{M_2}), \quad \text{for } t \leq t_0. \quad (\text{B.5})$$

647 Since $M_1(t_0) \geq 0$, there exists a non-negative solution $M_1(t) \geq M_1(t_0)e^{-\int (n_{M_1}T+e_{M_1}+r_{M_2})ds} \geq$
648 0 , for $t \in (t_0 - \epsilon_4, t_0 + \epsilon_4)$.

- 649 • From equation (3e):

$$\frac{dM_2}{dt} \geq M_2(n_{M_2}T - e_{M_2} - r_{M_1}), \quad \text{for } t \leq t_0. \quad (\text{B.6})$$

650 Since $M_2(0) \geq 0$, there exists a non-negative solution $M_2(t) \geq M_2(t_0)e^{\int (n_{M_2}T-e_{M_2}-r_{M_1})ds} \geq 0,$
651 for $t \in (t_0 - \epsilon_5, t_0 + \epsilon_5)$.

652 Therefore, the solution (T, H_1, H_2, M_1, M_2) of system (3) is nonnegative for $t \in [t_0, t_0 + \epsilon)$, with
653 $\epsilon = \min\{\epsilon_1, \epsilon_2, \epsilon_3, \epsilon_4, \epsilon_5\}$, which contradicts the initial assumption on t_0 . Therefore, the solution
654 remains non-negative for all time.

655 **Appendix C. Model non-dimensionalisation**

656 In the following, we present the non-dimensional versions of model (3) (since model (3) is a
657 generalisation of model (1), we choose not to present also the non-dimensional version of (1)).
658 Consider the following scaling for the variables and parameters that appear in these two models:

$$\begin{aligned}\bar{t} &= t \frac{a_{H_1} m_2}{m_1}, \quad \bar{H}_1 = \frac{H_1}{m_1}, \quad \bar{H}_2 = \frac{H_2}{m_1}, \quad \bar{M}_1 = \frac{M_1}{m_2}, \quad \bar{M}_2 = \frac{M_2}{m_2}, \quad \bar{T} = \frac{T}{\beta}, \\ a_1 &= \frac{a_{H_2}}{a_{H_1}}, \quad a_2 = \frac{a_{M_1} m_1^2}{a_{H_1} m_2^2}, \quad a_3 = \frac{a_{M_2} m_1^2}{a_{H_1} m_2^2}, \quad b_1 = \frac{p_{H_1} m_1}{a_{H_1}}, \quad b_2 = \frac{p_{H_2} m_1}{a_{H_1}}, \quad b_3 = \frac{p_{M_1} m_1}{a_{H_1} m_2}, \\ b_4 &= \frac{p_{M_2} m_1^2}{a_{H_1} m_2}, \quad e_1 = \frac{e_{H_1} m_1}{a_{H_1} m_2}, \quad e_2 = \frac{e_{H_2} m_1}{a_{H_1} m_2}, \quad e_3 = \frac{e_{M_1} m_1}{a_{H_1} m_2}, \quad e_4 = \frac{e_{M_2} m_1}{a_{H_1} m_2}, \\ r_1 &= \frac{r_{M_1} m_1}{a_{H_1} m_2}, \quad r_2 = \frac{r_{M_2} m_1}{a_{H_1} m_2}, \quad n_1 = \frac{n_{H_1} \beta m_1}{a_{H_1} m_2}, \quad n_2 = \frac{n_{H_2} \beta m_1}{a_{H_1} m_2}, \quad n_3 = \frac{n_{M_1} \beta}{a_{H_1}}, \quad n_4 = \frac{n_{M_2} \beta}{a_{H_1}}, \\ f_1 &= \frac{\alpha m_1}{a_{H_1} m_2}, \quad f_2 = \frac{g_{H_1} m_1^2}{a_{H_1} m_2}, \quad f_3 = \frac{g_{H_2} m_1^2}{a_{H_1} m_2}, \quad f_4 = \frac{g_{M_1} m_1}{a_{H_1}}, \quad f_5 = \frac{g_{M_2} m_1}{a_{H_1}}, \quad f_6 = \frac{f m_1}{a_{H_1} m_2}.\end{aligned}$$

After dropping the bar for simplicity, we obtain the following equations for the time-evolution of variables describing the tumour and immune cells (i.e., the non-dimensional version of model (3)):

$$\frac{dT}{dt} = f_1 T(1 - T) - f_2 H_1 T - f_3 H_2 T - f_4 M_1 T + f_5 M_2 T - f_6 T, \quad (\text{C.1a})$$

$$\frac{dH_1}{dt} = M_1 + b_1 H_1 M_1 (1 - H_1 - H_2) - n_1 H_1 T - e_1 H_1, \quad (\text{C.1b})$$

$$\frac{dH_2}{dt} = a_1 M_2 + b_2 H_2 M_2 (1 - H_1 - H_2) - n_2 H_2 T - e_2 H_2, \quad (\text{C.1c})$$

$$\frac{dM_1}{dt} = a_2 H_1 + b_3 M_1 (1 - M_1 - M_2) - n_3 M_1 T - e_3 M_1 + r_1 M_2 - r_2 M_1, \quad (\text{C.1d})$$

$$\frac{dM_2}{dt} = a_3 H_2 + b_4 M_2 H_2 (1 - M_1 - M_2) + n_4 M_2 T - e_4 M_2 - r_1 M_2 + r_2 M_1. \quad (\text{C.1e})$$

659 Since this non-dimensionalisation approach did not lead to a significant reduction in model pa-
660 rameters (i.e., the 31 parameters in model (3), were reduced to 25 parameters in model (C.1)),
661 we prefer to work with the original dimensional model. Moreover, while a sensitivity analysis
662 could be performed on the non-dimensional parameters shown above, such an analysis would
663 not shed light on the effect of original parameters/rates on tumour growth (especially since pa-
664 rameters such as m_1 and m_2 - important for the sensitivity of the original model - enter in various
665 combination terms that form the non-dimensional parameters).

666 **Appendix D. Bifurcation diagrams for the dominant immune responses**

667 Consider the ratios of the steady states M_1^*/M_2^* and H_1^*/H_2^* given by (2):

$$\frac{M_1^*}{M_2^*} = \frac{e_{H_1}H_1^*(a_{H_2} + p_{H_2}H_2^*(1 - \frac{H_1^*+H_2^*}{m_1}))}{e_{H_2}H_2^*(a_{H_1} + p_{H_1}H_1^*(1 - \frac{H_1^*+H_2^*}{m_1}))}, \quad (D.1)$$

$$\frac{H_1^*}{H_2^*} = \frac{(a_{M_2} + p_{M_2}M_2^*(1 - \frac{M_1^*+M_2^*}{m_2}))}{e_{M_2}M_2^* + r_{M_1}M_2^* - r_{M_2}M_1^*} (e_{M_1}M_1^* + r_{M_2}M_1^* - r_{M_1}M_2^* - p_{M_1}M_1^*(1 - \frac{M_1^*+M_2^*}{m_2})) \quad (D.2)$$

668 Numerical simulations show that, at the steady state, $M_1^* + M_2^* \approx m_2$ and $H_1^* + H_2^* \approx m_1$ (see
669 also Figures 6 and 7). In this case, the previous two ratios reduce to

$$\frac{M_1^*}{M_2^*} = \frac{e_{H_1}H_1^*a_{H_2}}{e_{H_2}H_2^*a_{H_1}}, \quad \frac{H_1^*}{H_2^*} = \frac{a_{M_2}(e_{M_1}M_1^* + r_{M_2}M_1^* - r_{M_1}M_2^*)}{e_{M_2}M_2^* + r_{M_1}M_2^* - r_{M_2}M_1^*}. \quad (D.3)$$

670 Solving the first equation in (D.3) for $H_1^*/H_2^* = (M_1^*/M_2^*)(a_{H_1}/a_{H_2})(e_{H_2}/e_{H_1})$, and substituting
671 this term into the second equation in (D.3), denoting by $M^* = M_1^*/M_2^*$, $r_M = r_{M_1}/r_{M_2}$ and
672 $a_H = a_{H_1}/a_{H_2}$, leads to the following second order equation in M^* :

$$a_H a_M \left(\frac{e_{H_2}}{e_{H_1}} \right) \left(M^* \frac{e_{M_2}}{r_{M_2}} + r_M M^* - M^{*2} \right) = \frac{e_{M_1}}{r_{M_2}} M^* - r_M + M^*. \quad (D.4)$$

673 If we fix r_{M_2} and vary r_{M_1} , we can graph implicitly M^* versus r_M versus a_H (or a_M), as shown in
674 Figure 5.

675 Consider now model (3). The case of the tumour-free steady state follows the previous case,
676 and the changes in the immune response as we vary a_{H_1}/a_{H_2} or r_{H_1}/r_{H_2} can be described again
677 by Figure 5.

678 Now, we focus on the steady state (4), and discuss the parameter range where this tumour-present
679 state exists. We look for solutions $T^* > 0$ of

$$\alpha - T^* \frac{\alpha}{\beta} - f - g_{H_1}H_1^* - g_{H_2}H_2^* - g_{M_1}M_1^* + g_{M_2}M_2^* = 0. \quad (D.5)$$

680 Using (4b)-(4d), we can replace H_1^* and H_2^* by M_1^* , M_2^* and T^* . Again we make the assumption
681 that $M_1^* + M_2^* \approx m_2$, $H_1^* + H_2^* \approx m_1$, as seen numerically for the steady state dynamics of these
682 models (see also Figures 10-11). Finally, re-writing $M_{1,2}^*$ in terms of m_2 and $M^* = M_1^*/M_2^*$ we
683 obtain the implicit equation (6), whose solution was graphed in Figure 8(a)-(c) (left panels) for
684 different values of g_{M_2} versus M^* . One could also graph g_{M_2} versus $H^* = H_1^*/H_2^*$ (right panels in
685 Figure 8), by considering the relation between the ratio of Th1 and Th2 cells in the presence of
686 tumour cells:

$$\frac{H_1^*}{H_2^*} = \left(\frac{M_1^*}{M_2^*} \right) \left(\frac{a_{H_1}}{a_{H_2}} \right) \left(\frac{n_{H_2}T^* + e_{H_2}}{n_{H_1}T^* + e_{H_1}} \right). \quad (D.6)$$

687 **Appendix E. Jacobian matrix for the immune and tumour-immune systems**

688 The Jacobian matrix associated with system (1) is:

$$J_1 = \begin{pmatrix} a_{11} & a_{12} & a_{13} & a_{14} \\ a_{21} & a_{22} & a_{23} & a_{24} \\ a_{31} & a_{32} & a_{33} & a_{34} \\ a_{41} & a_{42} & a_{43} & a_{44} \end{pmatrix} \quad (\text{E.1})$$

689 with

$$\begin{aligned} a_{11} &= p_{H_1} M_1^* \left(1 - \frac{H_1^* + H_2^*}{m_1}\right) - \frac{p_{H_1} H_1^* M_1^*}{m_1} - e_{H_1}, & a_{12} &= -\frac{p_{H_1} H_1^* M_1^*}{m_1}, \\ a_{13} &= a_{H_1} + p_{H_1} H_1^* \left(1 - \frac{H_1^* + H_2^*}{m_1}\right), & a_{14} &= 0, & a_{21} &= -\frac{p_{H_2} H_2^* M_2^*}{m_1}, \\ a_{22} &= p_{H_2} M_2^* \left(1 - \frac{H_1^* + H_2^*}{m_1}\right) - \frac{p_{H_2} H_2^* M_2^*}{m_1} - e_{H_2}, & a_{23} &= 0, & a_{24} &= a_{H_2} + p_{H_2} H_2^* \left(1 - \frac{H_1^* + H_2^*}{m_1}\right), \\ a_{31} &= a_{M_1}, & a_{32} &= 0, & a_{33} &= p_{M_1} \left(1 - \frac{M_1^* + M_2^*}{m_2}\right) - \frac{p_{M_1} M_1^*}{m_2} - e_{M_1} - r_{M_2}, \\ a_{34} &= -\frac{p_{M_1} M_1^*}{m_2} + r_{M_1}, & a_{41} &= 0, & a_{42} &= a_{M_2} + p_{M_2} M_2^* \left(1 - \frac{M_1^* + M_2^*}{m_2}\right), & a_{43} &= -\frac{p_{M_2} M_2^* H_2^*}{m_2} + r_{M_2}, \\ a_{44} &= p_{M_2} H_2^* \left(1 - \frac{M_1^* + M_2^*}{m_2}\right) - \frac{p_{M_2} M_2^* H_2^*}{m_2} - e_{M_2} - r_{M_1}. \end{aligned}$$

Figure E.16 shows the stability of the steady states exhibited by model (1) as we vary one

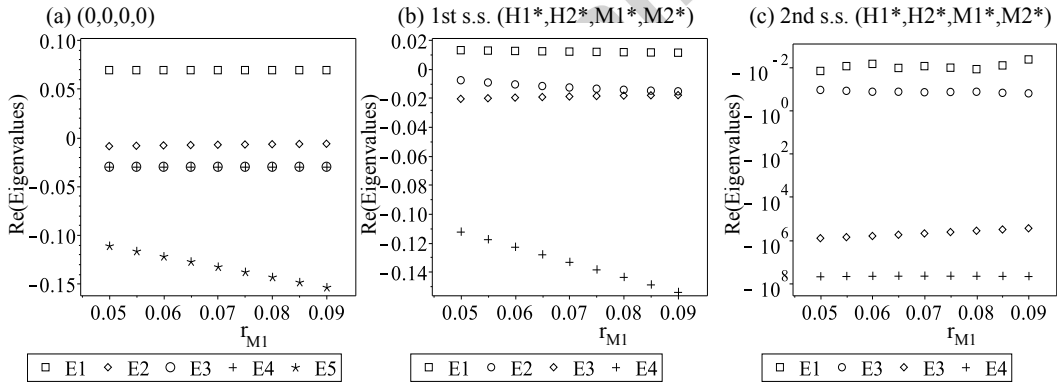


Figure E.16: Eigenvalues $E1 - E4$ of the Jacobian matrix (E.1) calculated at 3 different steady states: (a) Zero state $(0, 0, 0, 0)$; (b) first coexistence state $(H_1^*, H_2^*, M_1^*, M_2^*)$; (c) second coexistence state $(H_1^*, H_2^*, M_1^*, M_2^*)$. Here we assume that $a_{H_1} = a_{H_2} = 0.001$, $r_{M_2} = 0.05$ and $r_{M_1} \in [0.05, 0.09]$. The rest of parameter values are as described in Table A.1.

690

691 parameter. For simplicity, we chose parameter $r_{M_1} \in [0.05, 0.09]$ (but we note that we could
 692 have chosen any other parameter). The four symbols in Figure E.16 show the real parts of
 693 the four eigenvalues corresponding to the Jacobian matrix (E.1). Numerical calculations of the
 694 eigenvalues corresponding to the steady state $(0, 0, 0, 0)$ show that this state is stable for the
 695 parameter values shown in table A.1. In regard to the two immune coexistence steady states
 696 $(H_1^*, H_2^*, M_1^*, M_2^*)$ depicted in Figure 4: the state with low immune response (point (i) on Figure

697 4) is unstable, as shown in Figure E.16(b), and the state with high immune response (point (ii)
698 on Figure 4) is stable, as shown in Figure E.16(c).

699 We need to emphasise that these stability results depend strongly on all other parameter
700 values listed in Table A.1. As an example, in the following we show analytically how the stability
701 of the zero state $(0, 0, 0, 0)$ depends on the various parameters in the system. (While such an
702 analysis could be also performed for all other steady states, it is too complicated and beyond the
703 scope of this paper). The characteristic equation associated with $\det(J_{(0,0,0,0)} - \lambda \mathbb{I}) = 0$ is given
704 by

$$\begin{aligned} 0 &= (-e_{H_1} - \lambda) [(-e_{H_2} - \lambda)(p_{M_1} - e_{M_1} - r_{M_2} - \lambda)(-e_{M_2} - r_{M_1} - \lambda) + r_{M_1} r_{M_2} (e_{H_2} + \lambda) \\ &\quad - a_{H_2} a_{M_2} (p_{M_1} - e_{M_1} - r_{M_2} - \lambda)] + a_{H_1} [a_{M_1} a_{M_2} a_{H_2} - a_{M_1} (e_{H_2} + \lambda)(e_{M_2} + r_{M_1} + \lambda)] \\ &= F(\lambda). \end{aligned}$$

705 Note that this 4th order polynomial in λ (let us call it $F(\lambda)$) can have up to 4 real roots. For
706 $\lambda \rightarrow \pm\infty$, we have $F(\lambda) \rightarrow \infty$. If we can show that there are parameter values for which, at $\lambda = 0$
707 we have $F(0) < 0$, then it becomes clear that one root λ must be positive (and thus the zero-state
708 becomes unstable).

$$\begin{aligned} F(0) &= -e_{H_1} [(-e_{H_2})(p_{M_1} - e_{M_1} - r_{M_2})(-e_{M_2} - r_{M_1}) + r_{M_1} r_{M_2} (e_{H_2}) - a_{H_2} a_{M_2} (p_{M_1} - e_{M_1} - r_{M_2})] \\ &\quad + a_{H_1} [a_{M_1} a_{M_2} a_{H_2} - a_{M_1} (e_{H_2})(e_{M_2} + r_{M_1})] \end{aligned}$$

709 It is easy to observe that large r_{M_1} , r_{M_2} or p_{M_1} values can all lead to $F(0) < 0$. Figure E.17 shows
710 two possible parameter regions where $F(0) < 0$, thus ensuring that at least one eigenvalue λ of
711 the Jacobian matrix $J_1(0, 0, 0, 0)$ is positive and the zero state is unstable.

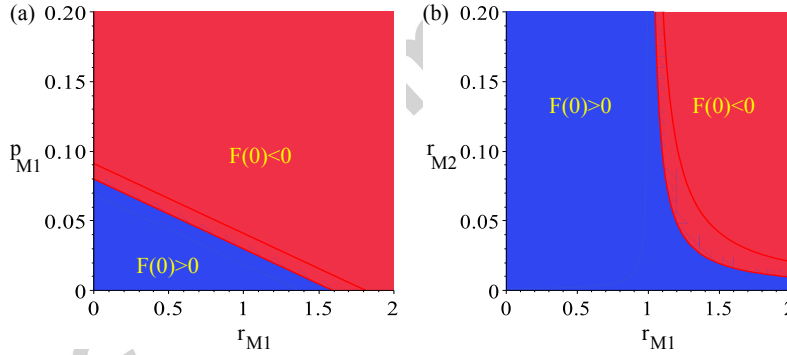


Figure E.17: Example of parameter regions where the steady state $(0, 0, 0, 0)$ can be unstable (i.e., $F(0) < 0$). (a) (r_{M_1}, p_{M_1}) plane; (b) (r_{M_1}, r_{M_2}) plane. All other parameters are kept fixed as in Table A.1.

712 The Jacobian matrix associated with system (3) is:

$$J_2 = \begin{pmatrix} b_{11} & b_{12} & b_{13} & b_{14} & b_{15} \\ b_{21} & b_{22} & b_{23} & b_{24} & b_{25} \\ b_{31} & b_{32} & b_{33} & b_{34} & b_{35} \\ b_{41} & b_{42} & b_{43} & b_{44} & b_{45} \\ b_{51} & b_{52} & b_{53} & b_{54} & b_{55} \end{pmatrix} \quad (\text{E.2})$$

713 with

$$\begin{aligned}
 b_{11} &= \alpha(1 - \frac{T^*}{\beta}) - \frac{\alpha T^*}{\beta} - g_{H_2} H_2^* - g_{M_1} M_1^* + g_{M_2} M_2^*, & b_{12} &= -g_{H_1}, & b_{13} &= -g_{H_2} T^*, \\
 b_{14} &= -g_{M_1} T^*, & b_{15} &= g_{M_2} T^*, \\
 b_{21} &= -n_{H_1} H_1^*, & b_{22} &= p_{H_1} M_1^* (1 - \frac{H_1^* + H_2^*}{m_1}) - \frac{p_{H_1} H_1^* M_1^*}{m_1} - e_{H_1} - n_{H_1} T^*, & b_{23} &= -\frac{p_{H_1} H_1^* M_1^*}{m_1}, \\
 b_{24} &= a_{H_1} + p_{H_1} H_1^* (1 - \frac{H_1^* + H_2^*}{m_1}), & b_{25} &= 0,
 \end{aligned}$$

714

$$\begin{aligned}
 b_{31} &= -n_{H_2} H_2^*, & b_{32} &= -\frac{p_{H_2} H_2^* M_2^*}{m_1}, & b_{33} &= p_{H_2} M_2^* (1 - \frac{H_1^* + H_2^*}{m_1}) - \frac{p_{H_2} H_2^* M_2^*}{m_1} - e_{H_2} - n_{H_2} T^*, \\
 b_{34} &= 0, & b_{35} &= a_{H_2} + p_{H_2} H_2^* (1 - \frac{H_1^* + H_2^*}{m_1}), \\
 b_{41} &= -n_{M_1} M_1^*, & b_{42} &= a_{M_1}, & b_{43} &= 0, & b_{44} &= p_{M_1} (1 - \frac{M_1^* + M_2^*}{m_2}) - \frac{p_{M_1} M_1^*}{m_2} - n_{M_1} T^* - e_{M_1} - r_{M_2}, \\
 b_{45} &= -\frac{p_{M_1} M_1^*}{m_2} + r_{M_1}, \\
 b_{51} &= n_{M_2} M_2^*, & b_{52} &= 0, & b_{53} &= a_{M_2} + p_{M_2} M_2^* (1 - \frac{M_1^* + M_2^*}{m_2}), & b_{54} &= -\frac{p_{M_2} M_2^* H_2^*}{m_2} + r_{M_2}, \\
 b_{55} &= p_{M_2} H_2^* (1 - \frac{M_1^* + M_2^*}{m_2}) - \frac{p_{M_2} M_2^* H_2^*}{m_2} - e_{M_2} - r_{M_1} + n_{M_2} T^*.
 \end{aligned}$$

3 coexistence states: (Ta,H1a,H2a,M1a,M2a), (Tb,H1b,H2b,M1b,M2b), (Tc,H1c,H2c,M1c,M2c)

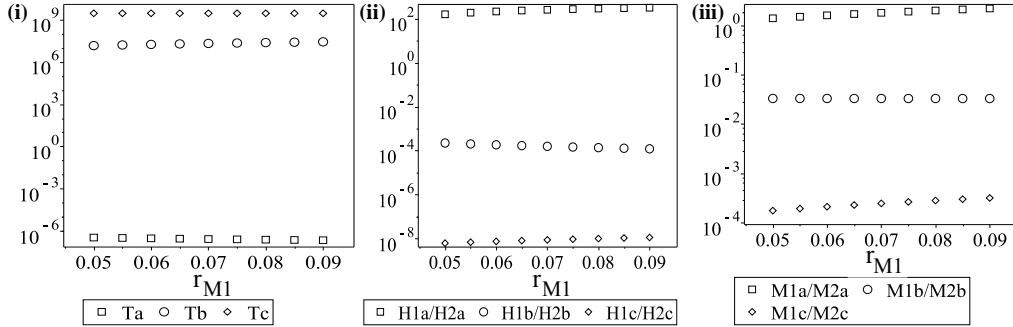


Figure E.18: There tumour-immune coexistence states (T^* , H_1^* , H_2^* , M_1^* , M_2^*) exhibited by model (3): (a) values of tumour sizes T^* ; (b) values of ratios H_1^*/H_2^* corresponding to the 3 tumours sizes depicted in (a); (c) values of ratios M_1^*/M_2^* corresponding to the 3 tumours sizes depicted in (a). Here we assume that $g_{M_2} = 2.3 \times 10^{-10}$, $g_{H_1} = 5 \times 10^{-9}$, $a_{H_1} = a_{H_2} = 0.001$, $r_{M_2} = 0.05$ and $r_{M_1} \in [0.05, 0.09]$. The rest of parameter values are as described in Table A.1.

715 Note that system (3) has: (i) one trivial steady state (0,0,0,0,0); (ii) one tumour-present,
 716 immune-absent state ($T^* = \beta - \beta f/\alpha$, 0, 0, 0, 0); (iii) two tumour-absent, immune-present states:
 717 (0, H_1^* , H_2^* , M_1^* , M_2^*), similar to those in model (1); (iv) three tumour-present, immune-present

718 states: $(T^*, H_1^*, H_2^*, M_1^*, M_2^*)$. As an example, we illustrate these three tumour-immune coex-
 719 sistence states in Figure E.18(a), as we vary parameter r_{M_1} , while keeping fixed $r_{M_2} = 0.05$,
 720 $a_{H_1} = 0.001$, $a_{H_2} = 0.001$, $g_{M_2} = 2.3 \times 10^{-10}$, $g_{H_1} = 5 \times 10^{-9}$ and all other parameters as in Table
 721 A.1. To have a better understanding of the immune responses during these three tumour sizes, in
 722 Figures E.18(b),(c) we also plot the ratios of H_1^*/H_2^* and M_1^*/M_2^* corresponding to each of these
 723 three coexistence states. Note that for these tumour-immune states, the very low tumour sizes
 724 (described by squares in Figure E.18(i)) occur in the presence of a type-I immune response (with
 725 $H_1/H_2 > 1$ in panel (ii), and $M_1/M_2 > 1$ in panel (iii)). In contrast, the very large tumour sizes
 726 occur in the presence of a type-II immune response.

727 Figure E.19 shows the stability of all steady states exhibited by model (3), (including the
 728 coexistence states discussed previously), as we vary parameter r_{M_1} and keep all other parameters
 729 fixed.

730 References

- 731 [1] P. Ehrlich, Ueber den jetzigen stand der karzinomforschung, *Ned Tijdschr Geneesk.* 5 (1909) 73–290.
 732 [2] J. Mattes, M. Hulett, W. Xie, S. Hogan, M. Rothenberg, P. Foster, C. Parish., Immunotherapy of cytotoxic T cell-
 733 resistant tumors by T helper 2 cells: An eotaxin and STAT6-dependent process, *Exp Med* 197 (3) (2003) 387–393.
 734 [3] Y. Xie, A. Akpınarlı, C. Maris, E. Hipkiss, M. Lane, E. Kwon, P. Muranski, N. Restifo, P. Antony., Naive tumor-
 735 specific $CD4^+$ T cells differentiated in vivo eradicate established melanoma, *The Journal of Experimental Medicine*
 736 207 (3) (2010) 651–667.
 737 [4] M. Kpbayashi, H. Kobayashi, R. Pollard, F. Suzuki, A pathogenic role of Th2 cells and their cytokine products on
 738 the pulmonary metastasis of murine B16 melanoma, *J. Immunol.* 160 (1998) 5860–5873.
 739 [5] P. Chen, Y. Huang, R. Bong, Y. Ding, N. Song, X. Wang, X. Song, Y. Lou, Tumor-associated macrophages promote
 740 angiogenesis and melanoma growth via adrenomedullin in a paracrine and autocrine manner, *Clin. Cancer Res.*
 741 17 (23) (2011) 7230–7239.
 742 [6] A. Mantovani, P. Romero, A. Palucka, F. Marincola, Tumour immunity: effector response to tumour and role of the
 743 microenvironment, *The Lancet* 371 (9614) (2008) 771–783.
 744 [7] G. Magombedze, S. Eda, V. Ganusov, Competition for antigen between Th1 and Th2 responses determines the tim-
 745 ing of the immune response switch during mycobacterium avium subspecies paratuberculosis infection in ruminants,
 746 *PLOS Computational Biology* (2014) 1–13.
 747 [8] D. Lucey, M. Clerici, G. Shearer, Type 1 and type 2 cytokine dysregulation in human infectious, neoplastic, and
 748 inflammatory diseases, *Clinical Microbiology Reviews* 9 (4) (1996) 532–562.
 749 [9] S. Romagnani, Th1/Th2 cells, *Inflamm. Bowel Dis.* 5 (4) (1999) 285–294.
 750 [10] A. Yates, C. Bergmann, J. V. Hemmen, J. Stark, R. Callard, Cytokine-modulated regulation of helper T cell popu-
 751 lation, *J. Theor. Biol.* 206 (4) (2000) 539–560.
 752 [11] C. Bergmann, J. L. van Hemmen, L. Segel, Th1 or Th2: how an appropriate T helper response can be made, *Bull.*
 753 *Math. Biol.* 63 (2001) 405–430.
 754 [12] M. Fishman, A. Perelson, Th1/Th2 differentiation and cross-regulation, *Bull. Math. Biol.* 61 (1999) 403–436.
 755 [13] F. Gross, G. Metzler, U. Behn, Mathematical modeling of allergy and specific immunotherapy: Th1-Th2-Treg
 756 interactions, *J. Theor. Biol.* 269 (1) (2011) 70–78.
 757 [14] Y. Kim, S. Lee, Y.-S. Kim, S. Lawler, Y. Go, Y.-K. Kim, H. Hwang, Regulation of Th1/Th2 cells in asthma
 758 development: A mathematical model, *Mathematical Biosciences and Engineering* 10 (4) (2013) 1095–1133.
 759 [15] Y. Louzoun, H. Atlan, I. Cohen, Modeling the influence of TH1- and TH2-type cells in autoimmune diseases, *J.*
 760 *Autoimmunity* 17 (4) (2001) 311–321.
 761 [16] M. Severins, J. Broughams, R. de Boer, The role of Th1/Th2 phenotypes in T cell vaccination: insights from a
 762 mathematical model, in: *T-cell vaccination*, Nova Science Publishers, Inc., 2008, pp. 139–158.
 763 [17] R. Eftimie, J. Bramson, D. Earn, Modeling anti-tumor Th1 and Th2 immunity in the rejection of melanoma, *Journal*
 764 *of Theoretical Biology* 265 (3) (2010) 467–480.
 765 [18] Y. Kogan, Z. Agur, M. Elishmereni, A mathematical model for the immunotherapeutic control of the Th1/Th2
 766 imbalance in melanoma, *Discrete and Continuous Dynamical Systems Series B* 18 (4) (2013) 1017–1030.
 767 [19] Y. Wang, T. Yang, Y. Ma, G. Halide, J. Zhang, M. Lindsey, Y.-F. Jin, Mathematical modeling and stability analysis
 768 of macrophage activation in left ventricular remodeling post-myocardial infarction, *BMC Genomics* 13 (2012) S21.
 769 [20] T. Yu, Design and validation of a mathematical model to describe macrophage dynamics in wound healing, Master’s
 770 thesis, Drexel University (2014).

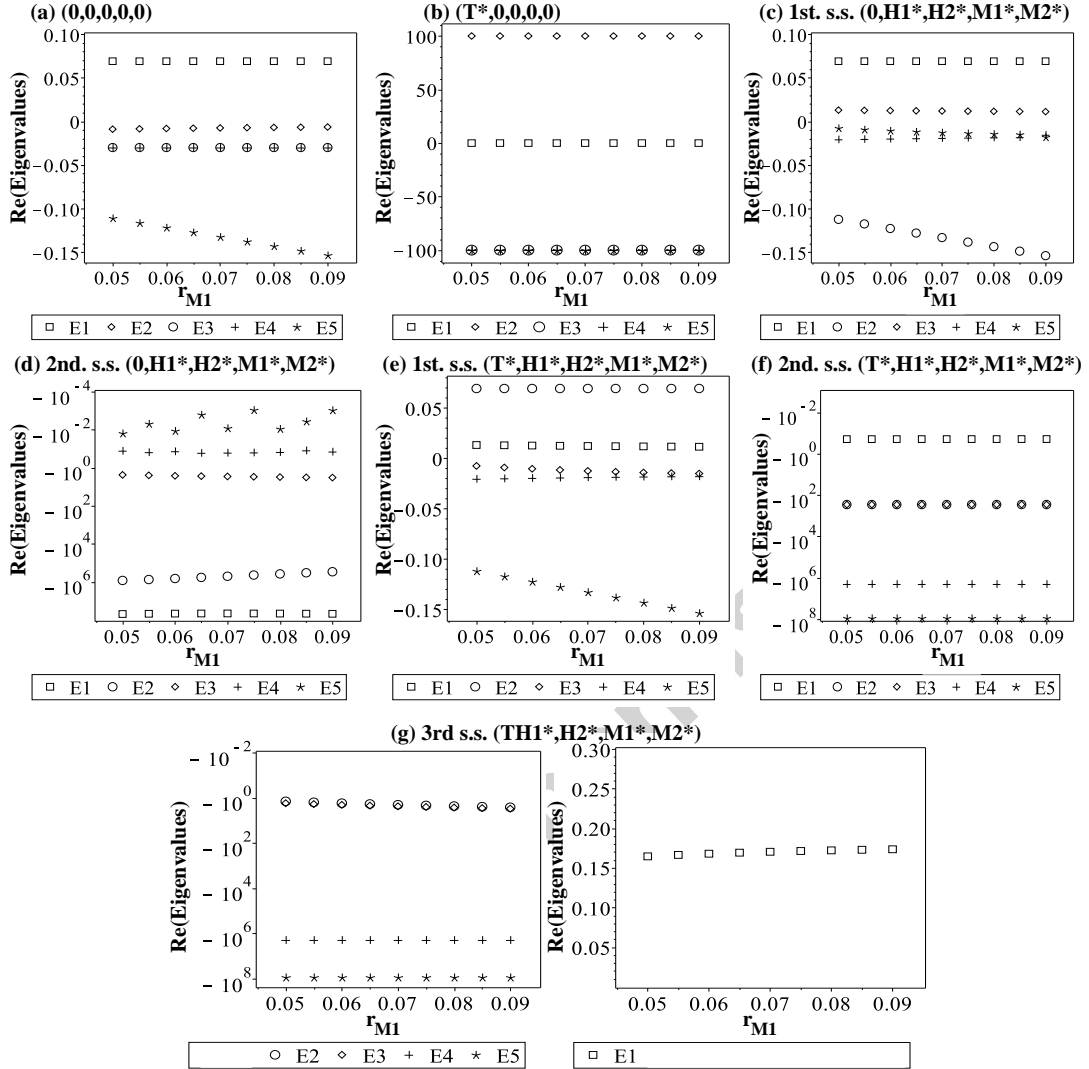


Figure E.19: The real part of eigenvalues E_1 - E_5 of the Jacobian matrix (E.1) calculated at 3 different steady states: (a) Zero state $(0,0,0,0,0)$; (b) Tumour-present, immune-absent state: $(T^* = \beta(1 - f/\alpha)^*, 0,0,0,0)$; (c),(d) Two tumour-absent, immune-present states: $(0, H_1^*, H_2^*, M_1^*, M_2^*)$; (e),(f),(g) Three tumour-immune coexistence states: $(T^*, H_1^*, H_2^*, M_1^*, M_2^*)$. Here we assume that $g_{M_2} = 2.3 \times 10^{-10}$, $g_{H_1} = 5 \times 10^{-9}$, $a_{H_1} = a_{H_2} = 0.001$, $r_{M_2} = 0.05$ and $r_{M_1} \in [0.05, 0.09]$. The rest of parameter values are as described in Table A.1.

- 771 [21] Y. Louzoun, C. Xue, G. Lesinski, A. Friedman, A mathematical model for pancreatic cancer growth and treatments,
 772 J. Theor. Biol. 351 (2014) 74–82.
 773 [22] N. den Breems, R. Eftimie, The re-polarization of M2 and M1 macrophages and its role on cancer outcomes, J.
 774 Theor. Biol. 390 (2016) 23–39.
 775 [23] C. Preue, H. Goebel, J. Held, O. Wengert, F. Scheibe, K. Irlbacher, A. Koch, F. Heppner, W. Stenzel, Immune-
 776 mediated necrotizing myopathy is characterized by a specific Th1-M1 polarized immune profile, The American

- Journal of Pathology 181 (6) (2012) 2161–2171.
- 777 [24] A. Taylor-Robinson, Inhibition of IL-2 production by nitric oxide: A novel self-regulatory mechanism for Th1 cell
778 proliferation, *Immunol. Cell Biol.* 75 (1997) 167–175.
- 779 [25] C. His, S. Macedonia, C. Tripp, S. Wolf, A. O'Garra, K. Murphy, Development of Th1 CD4⁺ T cells through IL-12
780 produced by *Listeria*-induced macrophages, *Science* 260 (1993) 547–549.
- 781 [26] J. Zhu, L. Guo, B. Min, C. Watson, J. Hu-Li, H. Young, P. Tschlis, W. Paul, Growth factor independent-1 induced
782 by IL-4 regulates Th2 cell proliferation, *Immunity* 16 (5) (2002) 733–744.
- 783 [27] S. Weisser, K. McLarren, E. Kuroda, L. Sly., *Methods in molecular biology: Generation and characterisation of*
784 *murine alternatively activated macrophages* (2013).
- 785 [28] L. Helming., *Inflammation: Cell recruitment versus local proliferation.*, *Current Biology* 21 (14) (2011) R548–
786 R550.
- 787 [29] E. Gauthier, S. Ivanov, P. Lesnik, G. Randolph, Local apoptosis mediates clearance of macrophages from resolving
788 inflammation in mice, *Blood* 122 (15) (2013) 2714–2722.
- 789 [30] P. Allavena, A. Mantovani, *Immunology in the clinic review series; focus on cancer: tumour-associated*
790 *macrophages: undisputed stars of the inflammatory tumour microenvironment*, *Clinical and Experimental Im-*
791 *munology* 167 (2012) 195–205.
- 792 [31] S. Jenkins, D. Ruckerl, P. Cook, L. Jones, F. Winkelman, N. van Rooijen, A. MacDonald, J. Allen, Local
793 macrophage proliferation, rather than recruitment from the blood, is a signature of Th2 inflammation, *Science*
794 332 (6035) (2011) 1284–1288.
- 795 [32] M. Panzer, S. Sitte, S. Wirth, I. Drexler, T. Sparwasser, D. Voehringer, Rapid in vivo conversion of effector T cells into
796 Th2 cells during helminth infection, *The Journal of Immunology* 118 (2) (2011) 615–623.
- 797 [33] C. Mills, K. Ley, M1 and M2 macrophages: the chicken and the egg of immunity, *J. Innate Immun.* 6 (6) (2014)
798 716–726.
- 799 [34] N.I.H., O.A.C.U., *Guidelines for endpoints in animal study proposals*,
800 [http://oacu.od.nih.gov/ARAC/documents/ASP Endpoints.pdf](http://oacu.od.nih.gov/ARAC/documents/ASP%20Endpoints.pdf) (1996).
- 801 [35] A. Laird, Dynamics of tumour growth, *Br. J. Cancer* 18 (3) (1964) 490–502.
- 802 [36] R. Wong, Apoptosis in cancer: from pathogenesis to treatment, *J. Experim. Clin. Res.* 30 (2011) 87.
- 803 [37] K. Knutson, M. Disis, Tumor antigen-specific T helper cells in cancer immunity and immunotherapy, *Cancer*
804 *Immunol Immunother* 54 (8) (2005) 721–728.
- 805 [38] M. Zhang, Y. He, X. Sun, Q. Li, W. Wang, A. Zhao, W. Di, A high M1/M2 ratio of tumour-associated macrophages
806 is associated with extended survival in ovarian cancer patients, *J. Ovarian Research* 7 (2014) 19.
- 807 [39] C. Lamagna, M. Aurrand-Lions, B. Imhof, Dual role of macrophages in tumour growth and angiogenesis, *J. Leuko-*
808 *cyte Biology* 80 (4) (2006) 705–713.
- 809 [40] A. Sica, P. Larghi, A. Mancino, L. Rubino, C. Porta, M. Totaro, M. Rimoldi, S. Biswas, P. Allavena, A. Mantovani.,
810 *Macrophage polarization in tumour progression*, *Seminars in Cancer Biology* 18 (5) (2008) 349–355.
- 811 [41] T. Yamaguchi, S. Fushida, Y. Yamamoto, T. Tsukada, J. Kinoshita, K. Oyama, T. Miyashita, H. Tajima, I. Ninomiya,
812 S. Munosue, A. Harashima, S. Harada, H. Yamamoto, T. Ohta, Tumor-associated macrophages of the M2 phenotype
813 contribute to progression in gastric cancer with peritoneal dissemination, *Gastric Cancer* 19 (4) (2016) 1052–1065.
- 814 [42] G. Solinas, G. Germano, A. Mantovani, P. Allavena. Tumor-associated macrophages (TAM) as major players of
815 the cancer-related inflammation, *J. Leukocyte Biology* 86 (2009) 1065–1073.
- 816 [43] H. Murphy, H. Jaafari, H. Dobrovolny, Differences in predictions of ODE models of tumor growth: a cautionary
817 example, *BMC Cancer* 16 (2016) 163.
- 818 [44] E. Sarapata, L. de Pillis, A comparison and catalog of intrinsic tumour growth models, *Bull. Math. Biol.* 76 (2014)
819 2010–2024.
- 820 [45] S. Benzekry, C. Lamont, A. Beheshti, A. Tracz, J. Ebo, L. Hlatky, P. Hahnfeldt, Classical mathematical models
821 for description and prediction of experimental tumour growth, *PLoS Comput. Biol.* 10 (8) (2014) e1003800.
- 822 [46] A. Talkington, R. Durrett, Estimating tumor growth rates in vivo, *Bull. Math. Biol.* 77 (2015) 1934–1954.
- 823 [47] M. Protti, L. D. Monte, Cross-talk within the tumor microenvironment mediates Th2-type inflammation in pancre-
824 atic cancer, *OncoImmunology* 1 (2012) 89–91.
- 825 [48] S. Friberg, S. Mattson, On the growth rates of human malignant tumours: implications for medical decision making,
826 *J. Surgical Oncology* 65 (1997) 284–297.
- 827 [49] M. Barros, F. Hauck, J. Dreyer, B. Kemkes, G. Niedobitek, Macrophage polarisation: an immunohistochemical
828 approach for identifying M1 and M2 macrophages, *PLoS One* 8 (11) (2013) e80908.
- 829 [50] T. Tatsumi, L. Kierstead, E. Ranieri, L. Gesualdo, F. Schena, J. Finke, R. Bukowski, J. Mueller-Berghaus, J. Kirk-
830 wood, W. Kwok, W. Storkus, Disease-associated bias in T helper type 1 (Th1)/Th2 CD4⁺ T cell responses against
831 MAGE-6 in HLA-DRB1*0401⁺ patients with renal cell carcinoma or melanoma, *J. Exp. Med* 196 (5) (2002)
832 619–628.
- 833 [51] M. Heusinkveld, S. van der Burg, Identification and manipulation of tumour associated macrophages in human
834 cancers, *J. Translat. Med.* 9 (2011) 216.
- 835

- 836 [52] D. DeNardo, J. Barreto, P. Andreu, L. Vasquez, D. Tawfik, N. Kolhatkar, L. Coussens, CD4⁺ T cells regulate
837 pulmonary metastasis of mammary carcinomas by enhancing protumor properties of macrophages, *Cancer cell* 16
838 (2009) 91–102.
- 839 [53] S. Almatroodi, C. McDonald, I. Darby, D. Pouniotis, Characterisation of M1/M2 tumour-associated macrophages
840 (TAMs) and the Th1/Th2 cytokine profiles in patients with NSCLC, *Cancer Microenviron.* 9 (1) (2016) 1–11.
- 841 [54] C. Roberts, A. Dickinson, L. Taams, The interplay between monocytes/macrophages and CD4⁺ T cell subsets in
842 rheumatoid arthritis, *Front. Immunol.* 6 (2015) 571.
- 843 [55] M. Wang, B. Yin, H. Wang, R.-F. Wang, Current advances in t-cell-based cancer immunotherapy, *Immunotherapy*
844 6 (12) (2014) 1265–1278.
- 845 [56] C. Voena, R. Chiarle, Advances in cancer immunology and cancer immunotherapy, *Discov. Med.* 21 (114) (2016)
846 125–133.
- 847 [57] F. Martinez, S. Gordon, The M1 and M2 paradigm of macrophage activation: time for reassessment, *F1000 Prime*
848 *Reports*.
- 849 [58] D. Hanahan, R. Weinberg, Hallmarks of cancer: the next generation, *Cell* 144 (2011) 646–674.
- 850 [59] B. Burkholder, R.-Y. Huang, R. Burgess, S. Luo, V. Jones, W. Zhang, Z.-Q. Lv, C.-Y. Gao, B.-L. Wang, Y.-
851 M. Zhang, R.-P. Huang, Tumor-induced perturbations of cytokines and immune cells networks, *Biochimica et*
852 *Biophysica Acta* 1845 (2014) 182–201.
- 853 [60] E. Flach, S. Schnell, Use and abuse of the quasi-steady-state approximation, *Syst. Biol.* 153 (4) (2006) 187–191.
- 854 [61] L. D. Monte, M. Reni, E. Tassi, D. Clavenna, I. Papa, H. Recalde, Intratumor T helper type 2 cell infiltrate corre-
855 lates with cancer-associated fibroblast thymic stromal lymphopoietin production and reduced survival in pancreatic
856 cancer, *J. Exp. Med.* 208 (2011) 469–478.
- 857 [62] A. Gliozzi, C. Guiot, R. Chinola, P. Delsanto, Oscillations in growth of multicellular tumour spheroids: a revisited
858 quantitative analysis, *Cell Proliferation* 43 (4) (2010) 344–353.
- 859 [63] J. Borghans, R. D. Boer, Quantification of T-cell dynamics: from telomeres to dna labeling, *Immunological Re-*
860 *views* 216 (1) (2007) 35–47.
- 861 [64] B. Asquith, J. Borghans, V. Ganusov, D. Macallan, Lymphocyte kinetics in health and disease, *Trends in Immunol-*
862 *ogy* 30 (4) (2009) 182–189.
- 863 [65] R. D. Boer, A. Perelson, Quantifying T lymphocyte turnover, *J. Theor. Biol.* 327 (2013) 45–87.
- 864 [66] D. Laydon, C. Bangham, B. Asquith, Estimating t cell repertoire diversity: limitations of classical estimators and a
865 new approach, *Phil. Trans. R. Soc. B* 370 (1675) (2015) 20140291.
- 866 [67] R. Eftimie, J. Gillard, D. Cantrell, Mathematical models for immunology: current state of the art and future research
867 directions, *Bull. Math. Biol.* 78 (10) (2016) 2091–2134.
- 868 [68] C. Danciu, A. Falamas, C. Dehelean, C. Soica, H. Radeke, L. Tudoran, F. Bojin, S. Pónzaru, M. Munteanu, A char-
869 acterization of four b16 murine melanoma cell sublines molecular fingerprint and proliferation behavior, *Cancer*
870 *Cell International* 13 (2013) 75. doi:10.1186/1475-2867-13-75.
- 871 [69] L. Cousins, Z. Werb, Inflammation and cancer, *Nature* 420 (2002) 860–867.
- 872 [70] S.-H. Lee, P. Starkey, S. Gordon, Quantitative analysis of total macrophage content in adult mouse tissues, *J. Exp.*
873 *Med.* 161 (1985) 475–489.
- 874 [71] Q. Wang, D. K. II, Z. Wang, CD8⁺ T cell response to adenovirus vaccination and subsequent suppression of tumor
875 growth: modeling, simulation and analysis, *BMC Systems Biology* 9 (2015) 27.
- 876 [72] D. Wodarz, Y. Iwasa, N. Komarova, On the emergence of multifocal cancers, *J. Carcinogenesis* 3 (2004) 13.
- 877 [73] H. Moore, N. Li, A mathematical model for chronic myelogenous leukaemia (CML) and T cell interactions, *J.*
878 *Theor. Biol.* 227 (2004) 513–523.
- 879 [74] J. Brown, L. Attardi, The role of apoptosis in cancer development and treatment response, *Nat. Rev. Cancer* 5
880 (2005) 231–237.
- 881 [75] K. Hung, R. Hayashi, A. Lafond-Walker, C. Lowenstein, D. Pardoll, H. Levitsky, The central role of CD4⁺ T cells
882 in the antitumor immune response, *J. Exp. Med.* 188 (12) (1998) 2357–2368.
- 883 [76] J. Wigginton, D. Kirschner, A model to predict cell-mediated immune regulatory mechanisms during human infec-
884 tion with *Mycobacterium tuberculosis*, *J. Immunology* 2001 (2001) 1951–1967.
- 885 [77] L. de Pillis, A. Radunskaya, C. Wiseman, A validated mathematical model of cell-mediated immune response to
886 tumor growth, *Cancer Res* 65 (17) (2005) 1916–1940.